JOURNAL OF GEOPHYSICAL RESEARCH, VOL. 103, NO. D14, PAGES 16,871–16,896, JULY 27, 1998

Water isotope module of the ECHAM atmospheric general circulation model: A study on timescales from days to several years

G. Hoffmann
Laboratoire des Sciences du Climat et de l'Environnement, CEA/CNRS, Centre d'Etudes de Saclay, Gif sur Yvette, France

M. Werner and M. Heimann
Max Planck Institut für Meteorologie, Hamburg, Germany

Abstract. Results are presented of a global simulation of the stable water isotopes $H_2^{18}O$ and $HD^{16}O$ as implemented in the hydrological cycle of the ECHAM atmospheric general circulation model. The ECHAM model was run under present-day climate conditions at two spatial resolutions (T42,T21), and the simulation results are compared with observations. The high-resolution model (T42) more realistically reproduced the observations, thus demonstrating that an improved representation of advection and orography is critical when modeling the global isotopic water cycle. The deuterium excess (d=δD-8*δ^{18}O) in precipitation offers additional information on climate conditions (e.g., relative humidity and temperature) which prevailed at evaporative sites. Globally, the simulated deuterium excess agrees fairly well with observations showing maxima in the interior of Asia and minima in cold marine regions. However, over Greenland the model failed to show the observed seasonality of the excess and its phase relation to δD reflecting either unrealistic source areas modeled for Greenland precipitation or inadequate description of kinetics in the isotope module. When the coarse resolution model (T21) is forced with observed sea surface temperatures from the period 1979 to 1988, it reproduced the observed weak positive correlation between the isotopic signal and the temperature as well as the weak negative anticorrelation between the isotopic signal and the precipitation. This model simulation further demonstrates that the strongest interannual climate anomaly, the El Niño Southern Oscillation, imprints a strong signal on the water isotopes. In the central Pacific the anticorrelation between the anomalous precipitation and the isotope signal reaches a maximum value of -0.8.

1. Introduction

Since more than a decade, a useful modeling tool in isotope geochemistry has been available: water isotope modules built into atmospheric general circulation models (AGCMs). The pioneering work was published by *Joussaume et al.* [1984]. For the first time, it presented the isotopic composition of precipitation under present-day climate conditions as modeled globally by an AGCM, the model of the Laboratoire de Météorologie Dynamique (LMD). Such isotope modules incorporate the well-known physics of fractionation of water isotopes into the hydrological cycle of AGCMs. The principal isotopic components of water are $H_2^{16}O$, $HD^{16}O$ (deuterium, approximately 0.5‰ of the water on the Earth), $H_2^{18}O$ ($\approx$ 2‰ of all water) and the radioactive tritium $HT^{16}O$(usually the isotopic composition of water is expressed as deviation from a standard, V-SMOW, the Vienna standard mean ocean water. For example, for $H_2^{18}O$, $\delta^{18}O = \left[(^{18}O/^{16}O)_{\text{Sample}}/(^{18}O/^{16}O)_{\text{V-SMOW}} - 1.\right]$ and, correspondingly, δD for $HD^{16}O$.). The isotopic composition of atmospheric water is a passive tracer and is influenced by a variety of climate parameters such as temperature, humidity and precipitation. Both the equilibrium fractionation of water isotopes during evaporation and the condensation [*Majoube*, 1971a, b] and kinetic, "nonequilibrium" effects [*Stewart*, 1975 ; *Jouzel and Merlivat*, 1984] are sufficiently known from laboratory experiments. AGCMs describe in detail the global hydrological cycle beginning with the evaporation from the ocean to condensation and precipitation, reevaporation and successive precipitation, and eventually continental runoff back to the ocean. Therefore the modeling

Paper number 98JD00423.
0148-0227/98/98JD-00423$09.00

task consists of calculating the fractionation during any phase transition releasing the vapor phase isotopically lighter compared to the liquid or solid phase. Finally, this gives us the simulated isotopic composition of vapor masses and of the corresponding precipitation.

This simple approach opens up a wide range of investigations in the areas of (1) testing and evaluating the hydrological cycle of AGCMs and (2) interpreting isotope signals on various timescales.

1. The hydrological cycle is certainly one of the most challenged parts of current climate models. Many processes are taking place on very small spatial scales (several kilometers or less), for example, convective cloud formation or continental river runoff. They have to be taken into account through their overall effect on the distribution of heat and moisture. The description of these processes on the still coarse numerical grid of today's AGCMs (several 100 km) is not straightforward, and hence this is where the art of parameterization comes in. Although the hydrological cycle itself is highly parameterized, the description of the isotope physics is based on first principles and does not introduce additional uncertain parameters, at least to first order. Therefore modeling water isotopes in an AGCM and comparing the results with global observations constitutes an important diagnostic tool for the evaluation of the hydrological cycle of these complex models.

2. Simple so-called Rayleigh models are the theoretical bases for the widespread use of isotopic records as a paleoproxy for temperatures as well as for the amount of precipitation. Such models consider an isolated air mass continuously cooled down to a certain temperature. Depending on the conditions at the evaporation site and at the condensation site, they calculate the isotopic composition of precipitation. Obviously, Rayleigh models largely simplify the complexity of atmospheric circulation; in particular, the mixing of air masses of different origin, the seasonality of precipitation, and the fraction of water vapor reevaporated from continental surfaces is not taken into account. AGCMs do include all these processes. Therefore they offer a physically much more complete modeling tool investigating the relations between the water isotopes and climate parameters on all timescales.

The general agreement between the results of AGCMs and observations was satisfying. The main characteristics of the global water isotope cycle were simulated by the AGCMs fitted until now with water isotope diagnostics, the LMD model, and the AGCM of the Goddard Instute for Space Studies (GISS) [*Jouzel et al.*, 1987]. Both models show a linear relation between the isotopes and the annual mean surface temperature in high latitudes (temperature effect), an increasing isotopic depletion of the precipitation in the interior of the continents (continental effect), and a linear relation between the precipitation and the isotopes mainly in the tropics (amount effect). However, there were also significant differences between the two models. The LMD model, for example, simulated the temperature effect only up to 0°C contrary to observations showing a linear relation up to 15°C. *Joussaume et al.* [1984] speculated that this problem was due to turbulent vertical mixing within the planetary boundary layer, a process included in the LMD model but not in the GISS. The latter calculated more realistically the observed spatial isotope-temperature relation but failed partially to show the correct seasonality of the water isotopes. Over Greenland a particularly important region for paleostudies, the surface temperatures simulated by the GISS model varied in agreement with observations, whereas the water isotopes showed virtually no seasonality. The results of both models are only compared with observations on the monthly to annual timescale.

In this paper we present simulation results from an isotope module implemented in the ECHAM general circulation model [*Modellbetreuungsgruppe*, 1994] under present-day climate conditions. We like to demonstrate the capacity of the ECHAM model to simulate the water isotopes on different timescales (days to interannual variations). Here we are particularly interested in processes that go beyond what we expect from simple Rayleigh models. Further, we like to figure out to what extent the water isotopes can be used to evaluate the hydrological cycle of the ECHAM model.

We analyze the annual mean and the seasonal cycle of the water isotopes by comparing them with the observations of the international atomic energy agency (IAEA) network. Over western Europe, where the number of isotope measurements is quite dense, these informations provide an almost complete picture of the isotopic composition in all components of the hydrological cycle (i.e. precipitation,vapor,groundwater,rivers). Such measurements can be used to test at least qualitatively the surface schemes of AGCMs over land. Using a river runoff model that is forced in an off-line mode by the output of the AGCM, we calculate the isotopic composition of large river systems. The seasonal cycle of water isotopes in rivers provides us with information on both the contribution of various catchment areas with different isotope signatures and the timing of processes like snowmelting. Subsequently, we compare the second-order quantity deuterium excess , i.e., the difference between ^{18}O and D , with observations. (the isotopic composition of most of meteoric water is found in a graph of δD versus $\delta^{18}O$ along the "Global Meteoric Water Line" (GMWL) [*Craig*, 1961]: $\delta D = 8 * \delta^{18}O + 10‰$; the deuterium excess d has been defined by *Dansgaard* [1964] as the difference $d = \delta D - 8 * \delta^{18}O$. Hence water on the GMWL has a deuterium excess of $+10‰$.) The deuterium excess of precipitation is usually assumed carrying information on the conditions prevailing at the evaporation site. Focusing on Greenland and western Europe, we discuss the model's ability to simulate source regions and pathways of water vapor under present-day conditions. Finally, we extend the investigated timescales to interannual and short-

term variations (<10 days). It is relevant to know to what extent even smaller interannual variations of the water isotopes are due to temperature, if one wants to use the isotopes as a sensitive indicator of a possible future climate change. On the other end of the timescale the study of short-term variations of the isotopes in water vapor gives us insights into synoptical and diurnal processes such as the position and frequency of storm tracks or the stability of the planetary boundary layer. In a forthcoming paper we will present our results on still longer timescales such as the climate conditions of the Holocene optimum (6 kyr B.P.) or the last glacial maximum (21 kyr B.P.).

2. Model Description and Simulation Experiments

The physics of fractionation of the water isotopes was built into the cycle 3 version of the ECHAM general circulation model which was developed in collaboration with the european center of midrange weather forecast (ECMWF) in Reading and the Max-Planck Institut für Meteorologie in Hamburg (for a full model description see *Modellbetreuungsgruppe* [1994]). In this study we analyze results of two spatial resolutions of this spectral climate model, the T42 and the T21 versions. These spectral truncation schemes correspond to a physical grid with a horizontal resolution of 2.8°×2.8°(time step of 24 min) and of 5.6°×5.6°(time step of 40 min), respectively. The model has 19 vertical layers from surface pressure up to a pressure level of 30HPa.

The water isotopes were implemented in a similar way as in the GISS AGCM [*Jouzel et al.*, 1987]. For each phase of "normal" water (vapor,cloud liquid water) being transported independently in the AGCM we define a corresponding isotopic counterpart. The isotopes and the "normal" water are described identically in the model as long as no phase transitions are concerned. Therefore the transport scheme both for active tracers (moisture, cloud liquid water) and for the corresponding passive tracers (moisture and the cloud water of the isotopes) is the semi-Lagrangian advection scheme according to *Rasch and Williamson* [1990]. It should be pointed out that contrary to the GISS model, the ECHAM allows also the treatment of the isotopic composition of cloud liquid water.

Here we present only a short summary of the fractionation processes focusing particularly on the introduced free parameters. The water isotopes ($H_2^{18}O$,$HD^{16}O$) are treated as separate forms of water, which are transported and transformed in parallel to bulk moisture in all aggregate states (vapor, liquid, and solid) as represented in the AGCM. Differences to bulk moisture arise only during transformation processes, where the water isotopes fractionate according to their different vapor pressures and their different diffusivities. Two types of fractionation processes are considered in the model: equilibrium and nonequilibrium processes. An equilibrium fractionation takes place if the corresponding phase change is slow enough to allow full isotopic equilibrium. On the other hand, nonequilibrium processes depend even on the velocity of the phase change and therefore on the molecular diffusivity of the water isotopes.

The first fractionation process comes to pass during the evaporation from the oceanic surface. We use the bulk formula

$$E_x = \rho C_v |\vec{v}_h| (1-k) (x_{vap} - \underbrace{\alpha (T_{Surf})^{-1} \beta R_{Oc} q_{sat}}_{x_{sat}}) \quad (1)$$

to describe the evaporative flux of the water isotopes. Here ρ is the density of air, C_v is the drag coefficient depending on the stability of the planetary boundary layer, $|\vec{v}_h|$ is the horizontal wind speed, x_{vap} is the mixing ratio of the water isotopes in the first layer, α is the equilibrium fractionation factor known from *Majoube* [1971], β is a factor considering a slight isotopic enrichment ($\approx 0.5‰$ for ^{18}O and 4 ‰ for deuterium respectively [*Craig and Gordon*, 1965]), of the oceanic surface due to evaporation, R_{Oc} is the isotope mass relation of the ocean corresponding to R_{SMOW}, and q_{sat} is the saturation mixing ratio. All nonequilibrium effects are included in the parameter 1-k taking into account the kinetics during the diffusion of vapor from a thin layer just above the ocean surface into the free atmosphere (for details see *Merlivat and Jouzel* [1979]). Dividing equation (1) by the corresponding vapor flux of bulk water $E = \rho C_v |\vec{v}_h| (q_{Vap} - q_{sat})$, we obtain the isotopic composition of the evaporative flux

$$\delta_E + 1 = \frac{(1-k)}{1-h} [\alpha (T_{Surf})^{-1} (\delta_{Oc} + 1) - (\delta_{Vap} + 1) * h] \quad (2)$$

with $\delta_{Oc} = \beta (R_{Oc}/R_{SMOW}) - 1$. Equation (2) clearly shows that the isotopic composition of the evaporative flux depends on sea surface temperature T_{Surf}, relative humidity h, and the δ value of vapor in the atmosphere δ_{Vap}. The latter is an independent quantity affected by the sum of all fractionation, transport, and evaporative processes. Therefore δ_{Vap} and δ_E differ at least on a regional scale and can only be assumed to be equal on a global scale [*Jouzel and Koster*, 1996].

Condensation either to ice or to liquid water is primarily described as an equilibrium process. The condensate either stays in isotopic equilibrium during the condensation (like small cloud droplets assuming a closed system:$R_{Con} = \alpha R_{Vap}$ with $R_{Con} = (x_{Con}/q_{Con})$ as the isotope relation in the condensate formed during one time step of the model and R_{Vap} as the relation in the corresponding vapor) or is instantaneously extracted (like ice crystals in open systems: $(dx_{Con}/dq_{Con}) = \alpha R_{Vap}$).

At very low temperatures (T <-20°C) a kinetic process becomes important, the diffusion of the isotopes through the oversaturated zone around the forming ice crystals. We consider this by replacing the equilibrium fractionation factor α_{eq} by an effective factor

$$\alpha_{eff} = \alpha_{eq}\alpha_{kin} \quad (3)$$

$$\text{with } \alpha_{kin} = \frac{S}{\alpha_{eq}\frac{D}{\hat{D}}(S-1)+1} \quad (4)$$

$(D/\hat{D})$ is the relation of the diffusivities between $H_2^{16}O$ and the heavier isotope (known from *Merlivat* [1978]) and S is the dimensionless oversaturation function parameterized by the temperature: $S = 1 - 0.003T$ (T is in °C; for a full discussion see *Jouzel and Merlivat* [1984]).

The kinetic processes occurring during the partial evaporation of raindrops into an undersaturated atmosphere below the cloud base are formulated in a similar manner as the fractionation during ice crystal formation. Instead of the oversaturation S depending in equation (4) on temperature, undersaturation is described in an analogous formula by the relative humidity below the cloud base, h_{eff}, depending on the humidity of the entire grid box (see *Stewart* [1975]).

The time a falling raindrop needs to adjust isotopically to its surrounding depends crucially on its size. Because there is no description of a drop size spectrum in the ECHAM model, we simply assume that convective showers produce primarily large drops equilibrating isotopically to only 45% , and large-scale clouds (like extratropical cyclones) produce smaller drops equilibrating nearly completely (95%).

We assume no fractionation during evaporation from land surfaces. Three different water reservoirs are described in the ECHAM model: a thin skin layer intercepting a certain fraction of the precipitation, a snow layer and a soil water pool. Water evaporates from the skin layer and from snow with the potential transpiration rate. Soil water evaporates either from the bare soil depending on the relative humidity or over vegetation depending on the photosynthetic activity of plants. It is known that evapotranspiration of plants does not change the isotopic composition of water taken up by roots [*Zimmermann et al.*, 1967; *Bariac et al.*, 1994a , b]. Furthermore, although it has been shown that the evaporation from bare soils is associated with a fractionation, other effects such as the "separation" of various isotope signals can strongly change the composition of the evaporative flux [*Gat*, 1981]: Depending on the state of the soil a certain fraction of precipitation is recycled back to the atmosphere, while some enters deeper layers and forms groundwater. Since these processes are not considered in sufficient detail in the simple soil water scheme of the ECHAM AGCM, we neglected to prescribe fractionation during evaporation from land in the present isotope module. This limitation must be kept in mind when interpreting the model results, since it has been shown that such fractionation processes can significantly influence the deuterium excess of continental precipitation [*Gat and Matsui*, 1991].

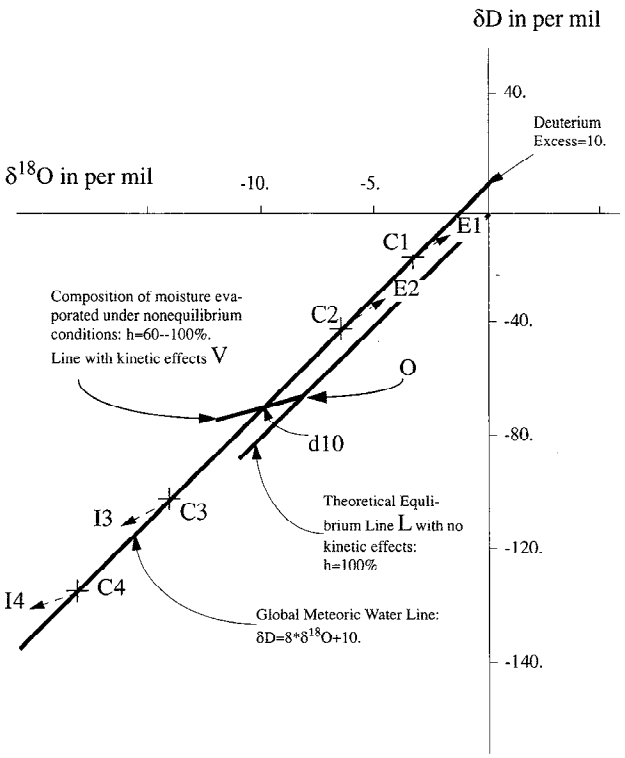

Figure 1. Scheme of kinetic, "nonequilibrium" processes adapted from *Dansgaard* [1964]. Without kinetic fractionation the isotopic composition of water vapor from the ocean would stay on the equilibrium line L corresponding to an excess of 0‰. Depending on the conditions during evaporation (relative humidity, temperature) the vapor moves, for example, from a point O with an excess of 0 ‰ along the line V (point d10 corresponds to 10‰ deuterium excess). If all condensation processes were equilibrium processes (assumed slope 1/8), the isotopic composition of precipitation would move along the global meteoric water line (GMWL) from the first condensate C1 to C4. Local processes can still change the excess: reevaporation of raindrops below the cloud (lowering the excess, E1 and E2) and kinetic formation of ice crystals at very low temperatures (enhancing the excess compared to the GMWL, I3 and I4).

We show here Figure 1 (adapted from *Dansgaard* [1964]) in order to clarify the role of the deuterium excess as a water tracer, carrying information on the conditions prevailing in the water source region, and thus to summarize all kinetic, nonequilibrium effects built into the model. If there were no kinetic effects (h=100%) the isotopic composition of the moisture evaporated from the ocean (point O in Figure 1) would lie on the equilibrium line L with a slope of $(\alpha_{18O}/\alpha_D) \approx 1/8$. The kinetic effect during evaporation (see equation (1)) which affects the $\delta^{18}O$ value more strongly than the δD value

changes the isotopic composition to a value somewhere on the line V. Depending on the relative humidity and the temperature, the evaporated moisture has a deuterium excess near the global mean value of d=10 ‰ (in the figure this global mean value lies at the point d10). If all condensation processes in the atmosphere would take place under equilibrium conditions with a constant relation of the fractionation factors of ^{18}O and D =1/8 (in fact, there are slight temperature dependent deviations from a constant relation) , the condensate (from the first condensate C1 to C4 in Figure 1) would lie on a line parallel to L. Therefore its deuterium excess d would not change. These mechanisms, although simplified in the scheme, give reasons for the use of d as a tracer for the climate conditions (relative humidity and temperature) at the evaporation site. However, the deuterium excess of the precipitation can be affected by two local effects. The evaporation of falling raindrops below the cloud results in a lowering of the excess (shown in Figure 1 by the shifts from C1 to E1 or C2 to E2). This nonequilibrium process occurs primarily under dry and hot conditions. On the other hand snow and ice formation at very low temperatures lead to a higher excess (shifts from C3 to I3 or C4 to I4).

The results discussed here are from a 5 year integration in T42 resolution (T42 control) and from a 10 year integration in T21 resolution (T21 control). Both simulations use climatological sea surface temperatures (SSTs) as lower boundary conditions, whereas a third simulation over 10 years in T21 resolution is forced with observed SSTs from the period 1979 to 1989.

3. Results

3.1. Modeled Climate

A full and detailed discussion of the global climate as modeled by the ECHAM3 model can be found in the work of *Roeckner et al.* [1992]. *Arpe et al.* [1994] and *K.Arpe and E.Roeckner* (Climate simulations: Impacts of increased greenhouse gases for Europe, submitted to *Advances in Water Research*, 1997) compare the hydrological cycle of the ECHAM model, which is of particular importance for our studies here with observations. We show the simulated 5 year mean 2m temperature (Figure 2a) and precipitation (Figure 2b) in order to give the reader at least an impression of the strength and weaknesses of the ECHAM's climate. Over the oceans the simulated 2m temperature is directly following the prescribed SSTs which are derived from observations. The simulated minimum temperature in the northern hemisphere is reached over Greenland (-33°C) and over East Antarctica in the southern hemisphere (-61°C). Both extremes are in good agreement with observations [*Putnins*, 1970; *Schwerdtfeger*, 1970]. The modeled seasonal temperature amplitude over land (not shown here) agrees fairly with temperature climatologies (July-January, East Antarctica: -35°C, Greenland 30°C, eastern Siberia: 45°C).

The modeled precipitation is much harder to validate by observed climatologies because over vast areas, in particular over the southern hemisphere oceans, there is a lack of data [*Jaeger*, 1976; *Legates and Willmott*, 1990]. Compared to former versions of the ECHAM model, the high-precipitation area within the tropical convergence zone is much better represented by the ECHAM3 version. The observed secondary minimum in tropical precipitation during DJF is well captured by the model. During JJA, such a minimum is not found in climatologies but still appears in the model. Thus in the annual mean the low-precipitation area in the tropical Pacific is slightly overestimated. The extent of regions with very small precipitation (less than 0.5 mm/d) in the subtropics seems to be too large compared with observations. This is primarily due to an overestimated strength of high-level convergence and subsequent subsidence in the subtropical highs. Generally, the subtropics appear somewhat too dry. In the southern hemisphere, monsoon type atmospheric circulation is too strong in the model. Therefore northern Australia and South Africa are too wet during DJF. There is a very good agreement between observed and simulated precipitation in the northern hemisphere storm track regions.

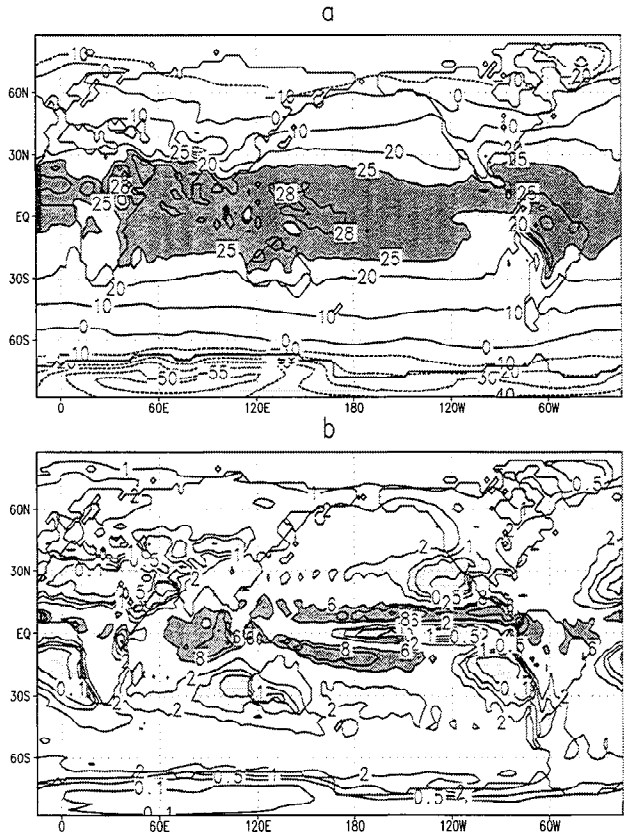

Figure 2. Five year mean of 2 m temperature in (a) degree Celsius , and precipitation in (b) mm/d, simulated by the ECHAM3 T42 version.

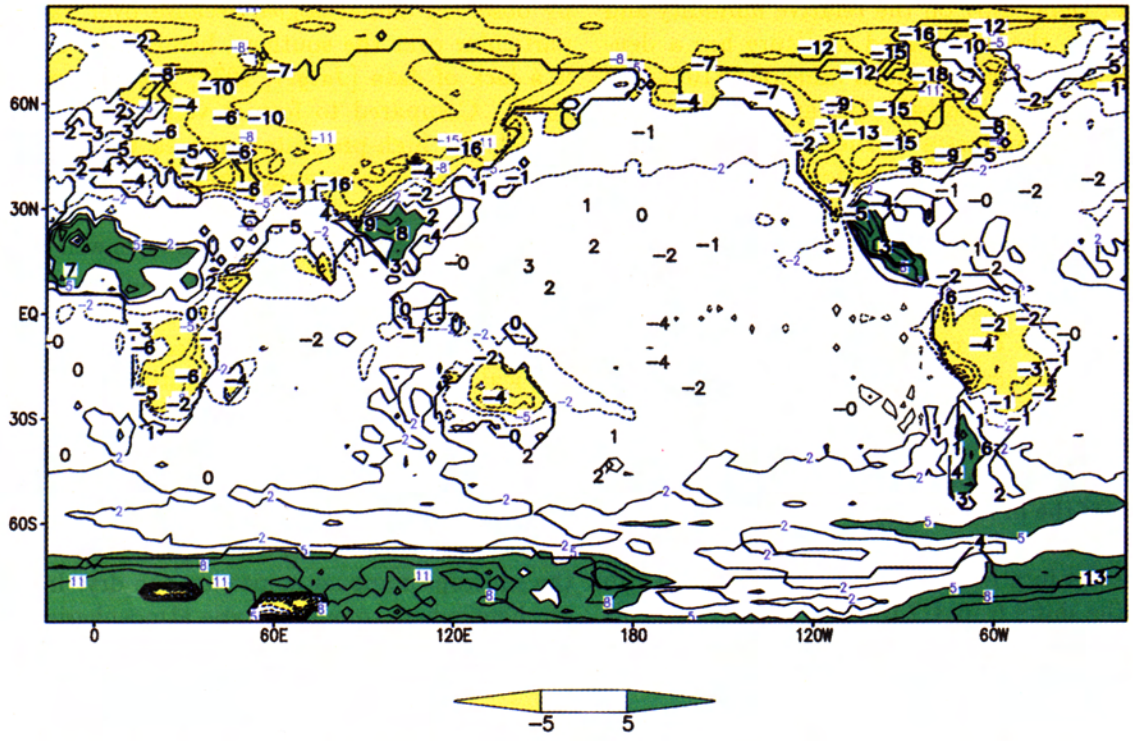

Plate 1. Annual mean of $\delta\,^{18}O$ in precipitation (in per mil) simulated by the ECHAM3 model (5 years T42-control) and IAEA station data [*IAEA*, 1992]. The bold numbers give the long-term means of the IAEA stations.

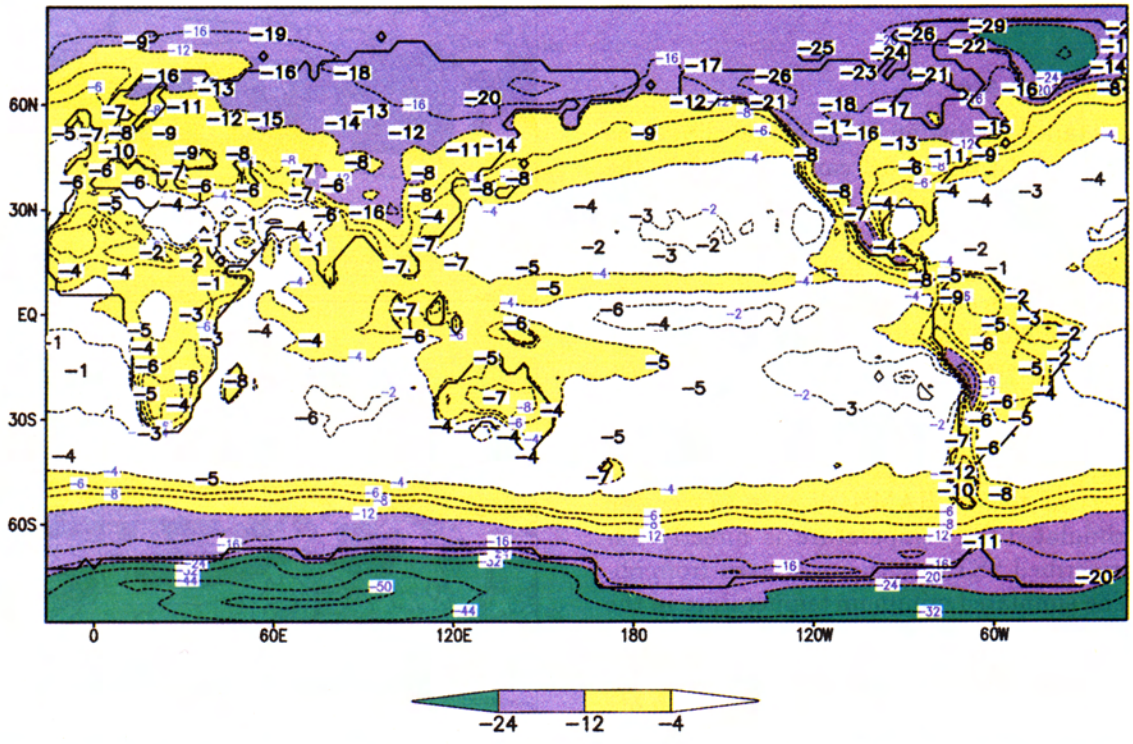

Plate 2. Seasonal cycle of $\delta\,^{18}O$ in precipitation (in per mil) defined as DJF-JJA values simulated by the ECHAM3 (5 years T42-control) model and IAEA observations. The bold numbers give the seasonal amplitude of IAEA stations with at least three seasonal cycles.

3.2. Annual Mean and Seasonal Cycle

In a first step, we compare our results for the water isotopes with observations of the IAEA. Plate 1 shows the annually averaged $\delta^{18}O$ values of precipitation of the T42-control simulation and of 153 stations selected from the IAEA database [*IAEA*, 1992]. All "classical" isotope effects already identified by *Dansgaard* [1964] are apparent in the figure: the temperature, the continental, the altitude, and the amount effect.

Cooling of air masses on their way to high latitudes leads to a successive detrainment of heavier isotopes and is responsible for the temperature effect. As a result of this process, the isotopic isolines are roughly parallel to the isotherms. This can clearly be seen over the southern hemisphere ocean south of 60° or over the North Atlantic where warm water of the Gulf Stream avoids a strong rainout of the air masses. This agrees well with observations, for example, the IAEA stations Reykjavik, $\delta^{18}O$=-7.8‰, and Isfjord, Spitzbergen, $\delta^{18}O$=-9.2 ‰, showing a heavy, "warm" isotope signal in precipitation compared with other marine stations at the same latitude.

In Plate 1, the continental effect appears as a pronounced land-sea contrast. The rainout of air masses itensifies when they are transported inland with the main circulation because further vapor supply from the open ocean is inhibited. This leads to a successive lowering of the $\delta^{18}O$ signal in precipitation. Such continental gradients are simulated by the model, for example, over western Europe or the eastern United States in accordance with the observations.

The rainout and the associated isotopic change of water vapor caused by elevation at orographic obstacles is called altitude effect [*Siegenthaler and Oeschger*, 1980]. The effect is difficult to document with the observations on the still coarse mesh of the IAEA network. Obviously, the ECHAM simulates such an isotope effect when air is lifted up at large mountain chains such as the Andes, the Rocky Mountains, or the Himalayas. If we exclude all observations over the ice sheets of Greenland and Antarctica we find a gradient of -0.13 ‰ $\delta^{18}O$ change per 100 m which is somewhat lower than the gradients of -0.16‰to -0.4‰ per 100 m found in regional studies [*Siegenthaler and Oeschger*, 1980].

The so-called amount effect is an inverse relationship between the amount of precipitation and its corresponding $\delta^{18}O$ value. It dominates in tropical and subtropical regions. Here air is frequently lifted in convective systems. As a consequence, the vertical rainout of air masses results in a corresponding isotope signal: Stronger convection produces more depleted vapor and therefore more depleted precipitation. The process resembles the high-latitude temperature effect but with a rainout taking place vertically instead of horizontally. In Plate 1, this effect is apparent mainly within the Intertropical Convergence Zone (ITCZ) where the band of strongest precipitation north and south of the equator appears as a region of comparable light isotopic composition of precipitation (between -4‰ and -7 ‰ over Indonesia). The geographical distribution and the strength of the amount effect are nicely corroborated by the observations on tropical islands (Truk, eastern Caroline Islands:-5.3‰), over Indonesia (Djakarta: -5.7‰ and Djajapura: -5.8 ‰) and New Guinea (Madang: -7.7‰).

The most obvious deficit of the simulated annual mean is the very strongly depleted rain over dry areas such as the Sahara or Central America. One part of the problem is defining an annual mean value for stations with only very few rainfall events recorded over a period of several years. Moreover, the model seems to overestimate the continental rainout in such areas (for example, -6‰ down to -9‰ in North Africa). Even now, we have no conclusive explanation for the poor model simulation in arid regions.

Plate 2 shows the calculated seasonal amplitude of $\delta^{18}O$ (expressed as the difference JJA-DJF), again allowing a comparison with the corresponding IAEA observations (we selected all stations with at least four measurements in any season). Obviously, there is no strong seasonality (i.e., a δ-amplitude > 5‰ (dark shaded) or < -5‰ (light shaded)) over the oceans where a continuous vapor source dampens extrema in the isotopic composition. On the other hand, the strongest seasonality is simulated in the interior of Siberia (-16‰) and North America (-12‰), only slightly underestimating the observed amplitude. The model results agree fairly well with the observed transition from a marine climate with a smooth isotope cycle to a continental climate with strong cycles. This holds both for a rather smooth transition such as over Europe where the westerlies transport air of marine origin far to the east and for a region with a rather strong gradient such as the eastern United States. Here isotopically depleted polar air builds up a very strong geographical gradient in winter.

Another interesting effect can be found in Plate 2. Regions with an amplitude <-5‰ (light shaded in Plate 2) correspond to the northern hemisphere temperature signal and region with an amplitude >5‰(dark shaded) to the southern hemisphere temperature signal. However in the tropics and subtropics the two signals appear in the opposite hemispheres. The region 0°–30°N shows the southern isotope signal and, vice versa, the region 0°–30°S, the northern signal. Monsoon type circulation is forced by differential insolation. Accordingly, the wet season takes place in the summer of the corresponding hemisphere. Because of the amount effect the most depleted rain is falling during (northern or southern) summer. At the edges of these regions (30°S–30°N) the temperature and the amount effect compete with each other. In the area of the southeastern monsoon the transition from a rather amount effect dominated region to a temperature effect dominated one is very sharp and, as far as the observations allow this

conclusion, quite well represented in the model (Plate 2). This holds also for the Amazon Basin where both parts of the basin, north and south of the equator, are influenced by the amount effect. The wet season of the northern part is shifted 6 months compared to the southern part, and therefore the seasonal signal is changing its sign within only some hundred kilometers from North to South (Plate 2). Although the simulated patterns seem to be correct, the model overestimates the isotopic seasonality by up to 4‰ in some regions dominated by the amount effect, such as Central and South America. A quantitative comparison of the model results with IAEA observations is provided by the correlations between $\delta^{18}O$ and temperature ("temperature effect"), $\delta^{18}O$ and precipitation ("amount effect"), and between $\delta^{18}O$ and δD ("GMWL"), both for the long-term means (spatial gradient of the means) and during the course of the year (spatial gradient of the seasonal amplitude DJF-JJA). These relationships are shown in Figures 3 and 4. For the modeled spatial gradients of the temperature effect and the the points shown represent all grid points of the model. In the other panels the model results include only grid points close to observation sites.

In Figures 3a–3c (temperature effect) the observations include measurements on snow samples from Greenland and Antarctica. Here the globally lowest $\delta^{18}O$ values have been measured at the top of the East Antarctic ice sheet (Vostok observed ≈-57‰, T42: -57‰) and over Greenland (Summit observed ≈-36 permill , T42: -34‰). The correlation of the water isotopes with the temperature below 15°C is almost the same in the simulations and in the observations (r=0.97 Obs; T42; T21). It breaks down at higher temperatures (T>15°C) where the amount effect controls the isotopic composition of rain. Both ECHAM simulations (T42 and T21) overestimate the isotope–temperature slope by about 10% (0.60‰/°C for T42 and 0.62‰/°C for T21 compared with 0.53‰/°C observed). At very low temperatures (T<-30°C), both the observations and the model results show an isotopic composition of precipitation slightly below the linear regression. Such a nonlinear behavior is already predicted by simple Rayleigh type models [*Jouzel and Merlivat*, 1984]. Its strength depends on the kinetic fractionation processes during the diffusive formation of ice crystals.

The amount effect only weakly appears as a global spatial gradient both in the observations and in the model results. Figures 3d–3f show the observations of all IAEA stations with an annual mean temperature of more than 15°C and the corresponding model results. Consequently, the points in Figures 3d–3f include stations from very different sites (continental, marine, etc.). Since the isotope variations due to the amount effect are much smaller (≈4‰) than the typical variations due to the temperature effect, one has to compare stations with similar climatic conditions. The dark squares in Figure 3d–3f mark sites from tropical islands where the amount of precipitation controls almost exclusively the isotopic composition. At least for these island stations the model and the observations show a similar spatial gradient of the amount effect (1.1‰ for

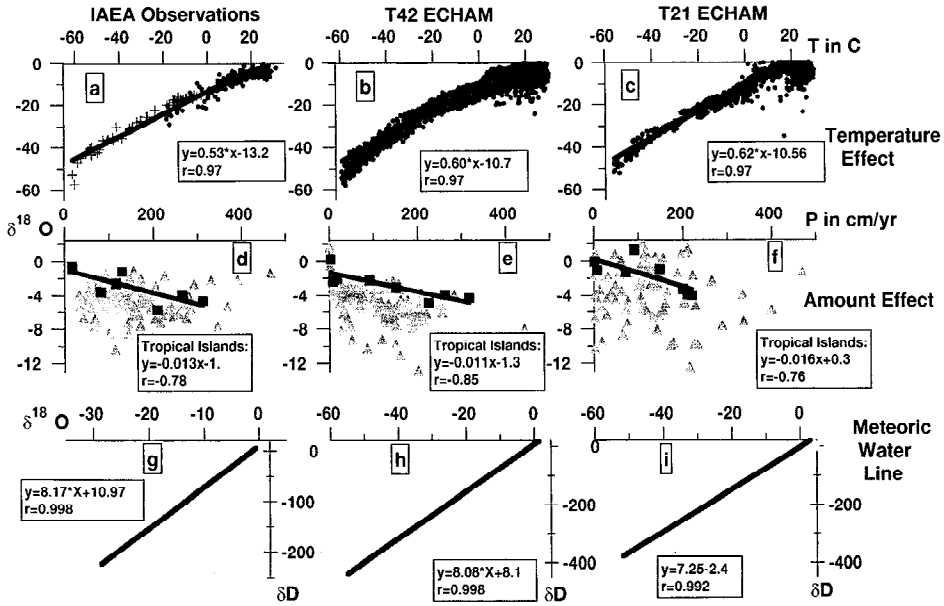

Figure 3. Spatial temperature-$\delta^{18}O$ (Figures 3a-3c), precipitation-$\delta^{18}O$ (Figures 3d-3f) and δD - $\delta^{18}O$ (Figures 3g-3i) relation for observations [*IAEA*, 1992], snow measurements adapted from *Jouzel et al.* [1987] (Fifures 3a,3d,3g), ECHAM3 T42-control run (Figures 3b,3e,3h), and T21-control (Figures 3c,3f,3i). For Figures 3b,3c,3h,3i the results from all model grid points are shown. In Figure 3e and 3f only results from grid squares with an IAEA station nearby are taken.

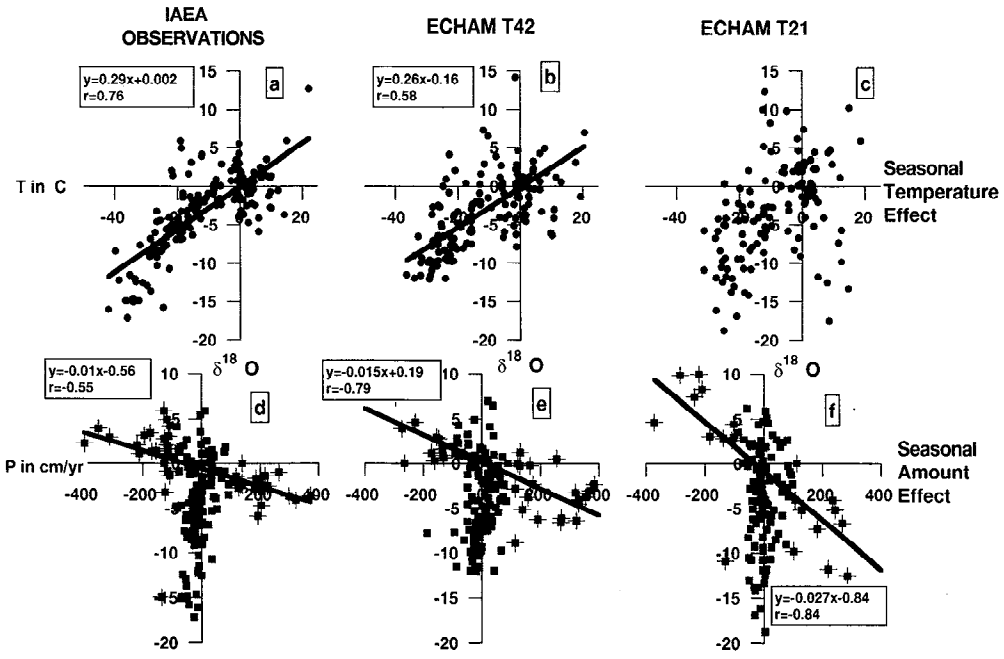

Figure 4. Seasonal (DJF-JJA) precipitation-$\delta^{18}O$ (Figures 4a-4c) and temperature-$\delta^{18}O$ (Figures 4d-4f) relation for the IAEA observations (Figures 4a,4d), ECHAM3 T42-control (Figures 4b,4e) and T21-control (Figure 4c,4f). Only model results are shown for grid squares with an IAEA station nearby. For the regression in Figure 4a,4b,4c only data (marked by a star) are considered whose seasonal amplitude of precipitation exceeds ±100 mm.

T42 and 1.6‰ for T21 compared to 1.3‰ observed per 100 cm annual precipitation).

In the T42-control run the global deuterium excess is underestimated by a global offset of 3‰, whereas the slope and the variance of the simulated is in perfect agreement with the observations (see Figures 3g–3i). In the T21-control run, the deviations from the are quite strong, in particular in the upper temperature range (between -10 and 0‰ $\delta^{18}O$). Probably the advective transport in the coarse resolution version is too diffusive to guarantee the parallelism of δD and $\delta^{18}O$.

The problems of the coarse resolution simulation are also apparent when considering the seasonality of the amount and the temperature effect (Figure 4). The spatial gradient of the seasonal amplitude (DJF-JJA) of the temperature–isotope relation ($\approx 0.3\frac{‰}{°C}$ in the observations and the T42 simulation) is about one half of the spatial gradient. This might be due to surface temperatures in the source region varying within the seasonal cycle simultaneously with the condensation temperatures. From Rayleigh models it is known that a change of evaporation temperatures, half as large as the temperature change at the site where the vapor condensates, flattens the seasonal $\delta^{18}O$-T slope by a factor of 2 [*Aristarain et al.*, 1986]. Nevertheless, the flattening of the seasonal slope can be explained by a more straightforward reasoning. The summer temperatures at many stations exceed 15°C where the temperature–isotope relation approximately starts to fail. This diminishes the seasonal amplitude of the water isotopes and thus flattens the seasonal slope in Figures 4a–4c. However, at locations where this effect is negligible, like in Antarctica, we found also a flattening of the modeled seasonal slope compared to the modeled spatial slope. This lead us to conclude that surface temperatures in the source region are indeed an important factor to explain the flattening of the seasonal slope. Although about 20% noisier (r being only 0.58 instead of 0.76 observed), the T42 simulation satisfactorily captures this observed feature.

Again, the T21 simulation is noisier (r=0.47) and appears describing the seasonality in the $\delta^{18}O$-T relation, worse than the high-resolution simulation. Under the assumption that the flattening of the slope is mainly caused by the changing temperature difference between vapor source and condensation site, the T21 version apparently has problems to simulate the source regions in the correct season. Therefore we attribute the overestimated variability of the seasonality to deficits of the seasonal transport in the model since the phenomena, depending on the annual mean conditions (mainly the temperature difference between the condensation and the evaporation site), are quite well simulated, as demonstrated in Figures 3a–3c).

The influence of the amount effect becomes more clear when seasonal variations of precipitation and the corresponding δ values are considered. In Figure 4d we plotted the seasonal amplitude (DJF-JJA) of precipitation and of $\delta^{18}O$ for all IAEA stations and the corresponding model results. If we exclude all stations

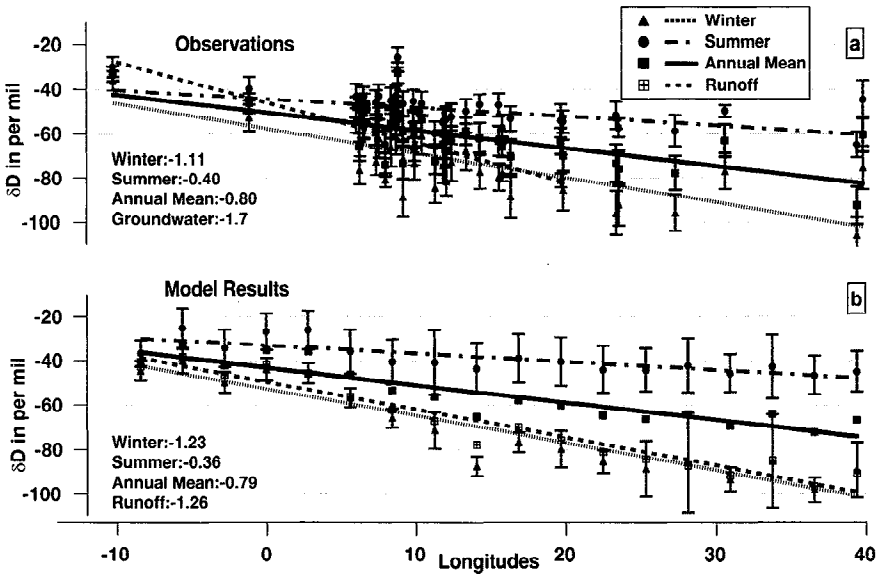

Figure 5. (a, top panel) IAEA observations and (b, bottom panel) ECHAM3 T42-control : continental gradient over Europe (from West to the East) of $\delta\,^{18}O$ in precipitation for summer (April-September), winter (October-May) and the annual mean. The model results (only land points are considered) are meridionally averaged from 45°N to 55°N and are shown from 10°W to 40°E. The isotopic composition of groundwater is taken from *Rozanski et al.* [1982]. Alpine stations are excluded because of their strong altitude effect.

with a small seasonality in precipitation (<100 cm/yr), we find a relationship of about 1‰ per 100 cm annual precipitation. In fact, the model overestimates the seasonality of the water isotopes in regions dominated by the amount effect (T42: 1.5‰ and T21: 2.7‰per 100cm/yr). This is a particular problem in tropical and subtropical regions where the model possibly overestimates the height of convection. If strongly depleted vapor at high altitude is mixed into the convective towers where the precipitation is formed, systematically very low δ values may result without considerably affecting the total amount of precipitation.

3.3. Surface Hydrology

Considering the coarse spatial resolution of present-day AGCMs, it is hardly possible to directly evaluate the performance of the model's surface schemes. The heterogeneity of natural land surfaces makes it difficult to derive boundary conditions for an AGCM model grid with a horizontal resolution of some hundred kilometers from observations (i.e., steepness of the orography, roughness of the surface, albedo, vegetation types and coverage, soil types). Given that these difficulties could be overcome, it is even harder to compare the simulated large-scale quantities (shortwave and longwave back scattering, fluxes of latent and sensible heat, runoff) with observations which are always biased by small-scale spatial or temporal variability. An approach to this problem is the use of a one-dimensional (1-D) version of the AGCM. Such a 1-D model version includes the physical parameterization of all AGCM subgrid processes adapted to the particular surface conditions of a point observation site. It is forced by observed temperature and shortwave radiation. Under the assumption that at least for some hours advective processes can be neglected, a direct comparison between the observed surface fluxes and the simulation results is possible. Although such efforts were quite successful [*Schulz et al.*, 1997], we would like to demonstrate here the potential of stable water isotope simulations to validate AGCM surface schemes on larger scales (temporal and spatial), without restricting the study on particular surface conditions.

In Figure 5b the simulated isotopic composition δD of precipitation over Europe (T42, meridionally averaged from 45°to 55°N) for summer (April-September) and winter (October-March) as well as the annual mean is shown as a function of longitude. The annual mean is influenced to approximately even parts by summer and winter precipitation. In correspondence to observations the model simulates no pronounced rainy season over Europe (at the 35 European IAEA stations, 54% of annual precipitation falls in summer compared to 50% modeled by the ECHAM) which otherwise would dominate the annual isotopic signal. In summer a large fraction of precipitation reevaporates from the surface and contributes to subsequent precipitation. Over Europe, evapotranspiration by plants dominates, compared with evaporation from bare soils. As plants do not fractionate the vapor transpired by their leaves against the water taken up by the roots, the isotopic depletion of water vapor is much weaker under warm conditions with a higher degree of water recycling than under cold con-

ditions. This process is an additional feedback mechanism to the temperature effect. In the interior of the continent it weakens still more the isotopic rainout than what is inferred from the higher summer temperatures. The simulated continental gradient of the water isotopes amounts to 0.36‰ δD per deg longitude eastward (observed 0.4‰ per deg) in summer and 1.23‰ per deg (observed 1.11 ‰ per deg) in winter. The model agrees fairly well with observations but shows a variability particularly in the interior of the continent of up to 20% higher than is observed.

Rozanski et al. [1982] developed a simple Rayleigh type model designed to explain the δ values of European precipitation. They showed a high sensitivity of the simulated isotopic signal on the reevaporation from the surface, which in their model is a prescribed quantity tuned optimally with respect to observations. In the ECHAM model, the evaporation flux from the surface E is an independent quantity calculated from prognostic variables. E mainly depends on temperature, vegetation coverage (prescribed higher than 80% over Europe), soil wetness, and stability of the planetary boundary layer. Therefore we conclude that at least over Europe the underlying assumptions made for the computation of the evaporation are supported by our isotope simulations. For a more quantitative validation of the surface processes by the water isotopes a detailed sensitivity study is necessary which relates changes of the surface parameters to calculated changes of the continental isotope gradient. Only such an analysis will reveal if the good agreement of the modeled and observed isotope gradient depends on the seasonally varying contribution of reevaporated water or is just a trivial result of the temperature effect.

Furthermore, studies investigating the isotopic composition of water in plants show a large spatial variability [*White et al.*, 1985; *White*, 1989; *Wang and Yakir*, 1995]. Trees located at dry sites take up water whose isotopic composition directly follows the most recent precipitation event. On the other hand, at wet sites, trees with long roots in contact with groundwater take up water which integrates the isotopic signal over several months. The simple bucket type surface scheme of the model averages spatially and temporally strongly varying conditions at the evaporation sites, at least over Europe in an approximately correct manner.

The Amazon Basin represents another region where detailed studies on the relation of the continental effect and recycling of water have been done [*Salati et al.*, 1979; *Gat and Matsui*, 1991; *Grootes et al.*, 1989]. Here the hydrological cycle runs much faster than over Europe. Moist air masses are advected by the trade winds from the tropical Atlantic westward into the basin and rainout in convective systems. The amount of water vapor which reevaporates isotopically unchanged from the tropical rain forest is very large throughout the year. From the observed mean isotopic gradient of 0.083‰ per degree longitude (to the West) it has been estimated that in the annual mean, about 40% of the advected vapor leaves the basin again in vapor form. This percentage undergoes large seasonal variations between 0 and 90% [*Grootes et al.*, 1989]. The ECHAM model also simulates, compared to Europe, a much weaker spatial gradient of 0.089‰ per in the Amazon Basin, indicating that the model predicts approximately the correct contribution of locally evaporated vapor to the precipitation in that region.

Moreover, the water isotopes bear the potential to test also other components of the hydrological cycle over land. The dotted line in Figure 5a (adopted from *Rozanski et al.* [1982]) shows a rough estimate of the mean isotopic composition of European groundwaters (for the database see also *Rozanski* [1985]). At least in central Europe it is more influenced by winter precipitation. Groundwater formation is supposed to dominantly take place under winter conditions when the soils are wet and saturated. Moreover, a much smaller part of the precipitation reevaporates during winter. The dotted line in Figure 5b shows the simulated δD value of the modeled runoff which represents both the direct surface runoff (i.e., rivers) and the water available for groundwater formation, as represented in ECHAM's simple surface scheme. The isotopic composition of the ECHAM's runoff is very close to the winter precipitation, indicating that the simulated groundwater recharge mainly takes place in wintertime. This indirect inference is confirmed by analyzing the seasonality of the modeled runoff itself. Indeed, 75% of the model's annual runoff in Europe is formed in wintertime.

Rivers are another important component in the global hydrological cycle. They transport back to the ocean all the continental precipitation that is not captured in internal drainage basins such as the Sahara or the Great Salt Lake region in the United States. Studies on the isotopic composition of river water published so far mainly focus on the mixing of different isotope signals of tributary rivers at their confluence (for example, *Fritz* [1981] discusses observations from the Rhine, Mackenzie, Mississippi and the Amazon Rivers). Unfortunately, systematic measurements over several years are, at least to the author's knowledge, not yet available. The δ value of river water is influenced by a number of factors. The most important is the isotopic composition of precipitation in the catchment area. Other processes become important for the understanding of the seasonal cycle of the isotopes in rivers such as the onset of snowmelting (snow being of course highly depleted), the amount of surface runoff determined by soil conditions (wet or dry), and reevaporation or evaporative enrichment of river water under warm and dry conditions. From the modeler's point of view the crosscheck of the simulated river runoff with the isotopes provides the possibility to test these mechanisms.

AGCM's river runoff into the ocean was already calculated in order to fully couple atmospheric and oceanic GCMs [*Russell and J.R.Miller*, 1990; *Sausen et al.*,

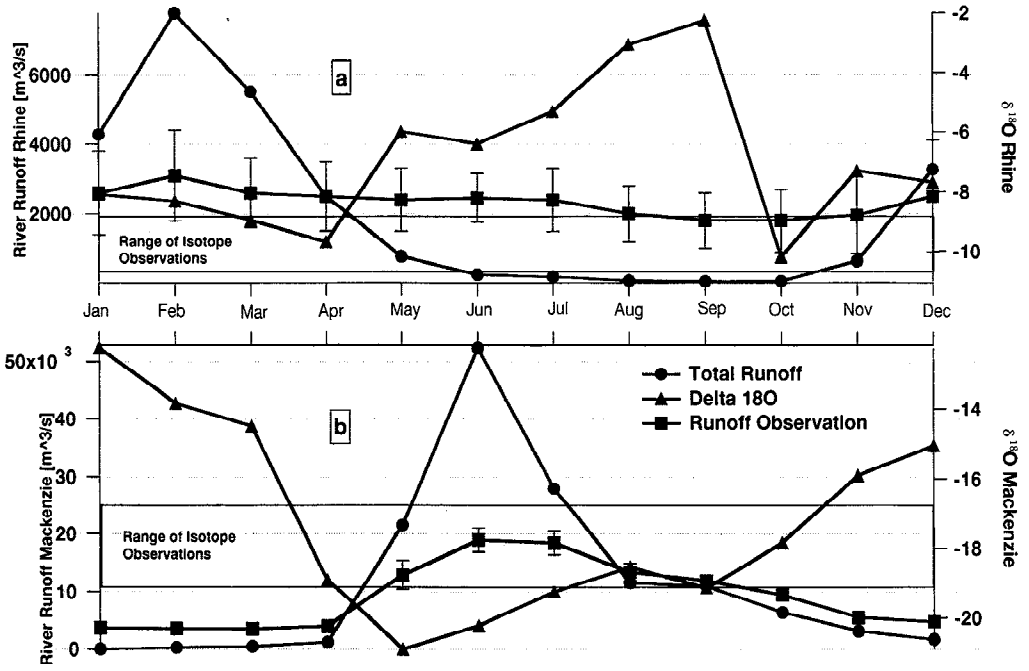

Figure 6. ECHAM3 T42-control and observations: River runoff (in m^3/s) and its isotopic composition (in per mil) of the rivers (a) Rhine and (b) Mackenzie (the observations of the runoff are from the Global Runoff Data Center (GRDC) network [*Dümenil et al.*, 1993], the observed range of isotope observations is taken from *Fritz* [1981] and *Hitchon and Krouse* [1972]). For details of the calculation of the runoff see the Appendix.

1994]. We use here the river runoff scheme of *Sausen et al.* [1994] calculating both the total amount of runoff at the mouth of individual rivers and its isotopic composition. The scheme uses the runoff simulated by the AGCM at every grid box and calculates off-line the transport by rivers according to the slope of the orography (for details, see the Appendix). No fractionation by evaporative enrichment is taking into account in calculating the isotopic composition of river water. At least for the Rhine and Mackenzie Rivers, these effects are assumed to be negligible. In Figure 6 we show for both rivers the observed and the modeled seasonal cycle of river runoff (in m^3/s) and its modeled isotopic composition.

The observed runoff of the Rhine shows only a weak seasonal amplitude with a maximum in late winter and a minimum in late summer. Its runoff originates primarily from water of two different source regions, a lower basin extending north of Basel up to the mouth of the Rhine and an alpine basin. These two areas differ strongly in their isotopic signature of -6 to -7‰ for the lower basin and of -12 to -14‰ for the higher alpine basin [*Fritz*, 1981]. The runoff scheme approximately predicts the observed annual mean runoff of about 3000 m^3/s. However, even if we consider that the observed, quite flat seasonality of the Rhine's outflow might partly result from anthropogenic influences (such as river regulation), the model strongly overestimates its seasonality. This model weakness was already noted by *Sausen et al.* [1994]. It could at least partly be due to problems of the ECHAM surface scheme simulating locally too much runoff when the soils are wet and too few by drainage if the soils are rather dry. A further problem of the present river runoff scheme is that the amount of runoff critically depends on the exact size and location of the river catchment area, which is difficult to define in the coarse resolution ($\approx$ 250×250km) used here.

The modeled annual mean isotope value of the Rhine's runoff is about -8‰. This fits quite well to measurements of Rhine water made in the Netherlands. The measured low isotope values of -10.5‰ in summer and -8.8‰ in winter have been interpreted by a high fraction of alpine meltwater during summer ($\approx$50%) and a comparable low fraction during winter ($\approx$20%, see *Fritz* [1981]). The most depleted water at the Rhine's mouth is modeled already during late spring, when depleted alpine water (in the mean is about 1‰ more depleted than the runoff from the lower basin) contributes stronger to the river outflow (60% compared to 30% otherwise). Analyzing the varying contribution of the two basins to the total outflow, we could not find a higher summer contribution of alpine water to the Rhine's outflow. Both catchment areas nearly dry up in summer (July-October) making the calculation of a reliable isotope content of the river outflow difficult. The problems of the model's surface scheme (see above) obviously do not only lead to a largely overestimated seasonal amplitude of the outflow itself but also disturb a realistic representation of the two catchment areas with their different isotope signature. However,

for a detailed check of the model results, isotope measurements at several places along a river are needed to distinguish the different catchment areas by their isotopic signals.

For the Mackenzie river, a large Arctic river with a catchment area extending over the entire canadian Northwest Territories, the river runoff scheme calculates again an overestimated seasonal amplitude of the river runoff (Figure 6). The outflow is too strong in summer and too weak in winter. The weighted mean δ value is -19‰, which is in fair agreement with observed δ values between -17‰and -21‰[*Hitchon and Krouse*, 1972]. The isotope values and the amount of runoff are anticorrelated over the seasons. This is typical for arctic rivers which are strongly affected by meltwater during the short summer period.

In the tropics, isotope observations of river water are rare. For the Amazon the model computes a significantly underestimated annual mean δ value of ≈-10 to -11‰ as compared to the observed ≈-5 to -6‰, although the simulated isotopic composition of precipitation in the Amazon Basin appears to be correct (see Plate 1). This deficit, i.e., the fact that the runoff is clearly more depleted than the precipitation in the catchment area, is typical for all modeled tropical rivers. Apparently, the model's runoff consists predominantly of rain from strong convective events. During strong rainfall the soil buckets in the model fills up rapidly and any further precipitation is added to the runoff. Because of the amount effect, such precipitation is strongly depleted and therefore dominates the mean runoff. Certainly, such a strong separation of soil wetness and runoff is unrealistic, and the model should be improved by allowing diffusive mixing between the reservoirs before the runoff leaves the system.

3.4. Deuterium Excess

In Plate 3 we compare the annual average of the simulated deuterium excess with observations. Value d, defined as the mass-weighted difference between $\delta^{18}O$ and δD, does not show its dependence on temperature or precipitation. Besides local phenomena as the reevaporation of raindrops and as the formation of ice crystals in oversaturated air, the annual d values of precipitation reflect the mean conditions prevailing in the region of the corresponding vapor source. The globally highest deuterium excess is measured in the Near and Middle East (Alexandria, Egypt: 16.3‰; Aleppo, Syria: 17.5‰; Bet Dagan, Israel: 18.2‰; Kabul, Afghanistan: 18.6‰). *Gat and Carmi* [1970] suggested that in particular the conditions over the Mediterranean and the Kaspian Seas are responsible for the high d-values. There, the evaporation takes place under extreme nonequilibrium conditions because dry and comparatively cold continental air is overlaying warm surface water. The ECHAM simulates the globally highest excess in this region, reaching a maximum of 21‰ over Tibet. Since the model is not yet fit with the capacity to tag water, we cannot confirm that the pro-

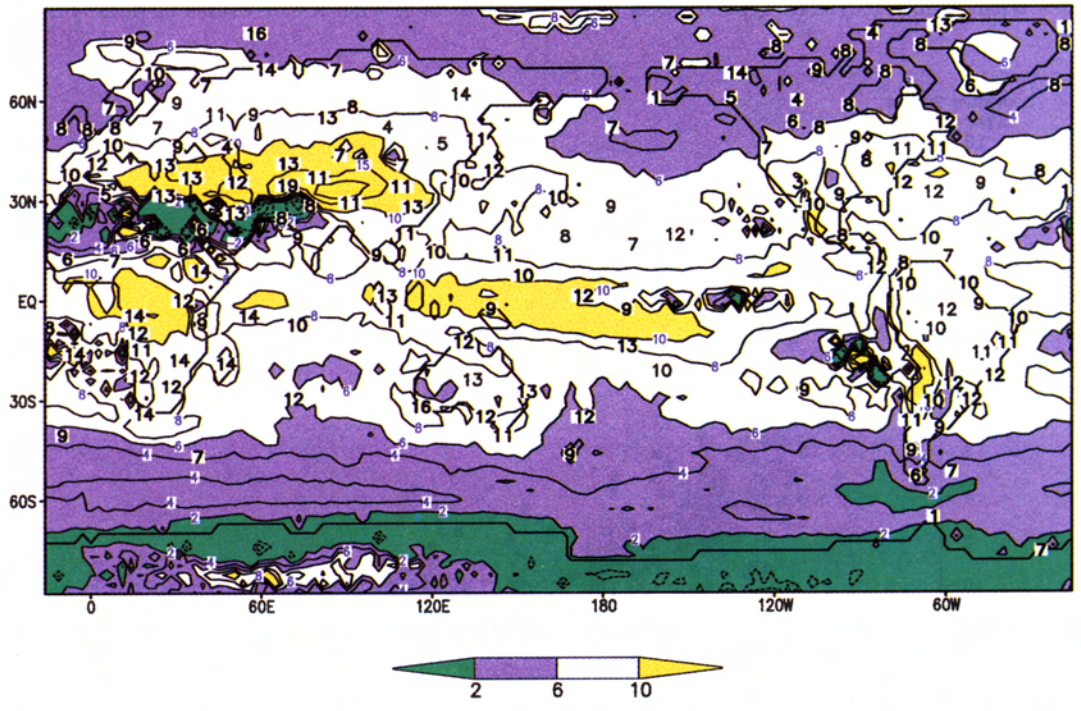

Plate 3. Annual mean of the deuterium excess (in per mil) in precipitation simulated by the ECHAM3 model (5 years T42-control) and observations from IAEA stations [*IAEA*, 1992]. The bold numbers give the long term means of the IAEA stations.

posed mechanism produces such high excess values also in the model. In the annual mean the vapor above the Mediterranean and the Kaspian Seas does not show particular high deuterium excess. For a detailed analysis we need information on different vapor source regions and the corresponding isotopic composition.

Nearly everywhere else, the model underestimates the deuterium excess by about 2–4‰. As first sensitivity studies with the ECHAM model demonstrated, the global mean excess value is strongly affected by the function $(1 - k)$ of equation (1). Thus a tuning of this function should be possible in order to get a more correct agreement with the . Although k is far from being a "free" parameter, its functional dependence on the wind velocity was taken from a globally averaged one-dimensional model [*Jouzel and Merlivat*, 1984] and can certainly be modified in the AGCM.

Another deficit of the simulated deuterium excess is the astonishing high variability in the marine regions of the subtropical highs. This again is, such as for the rainfall over the Sahara, at least partly a consequence of the poor statistic in regions where only a few precipitation events determine the annual signal. There, the annual mean δ-value and the seasonal cycle already show quite a high spatial variability (Plate 1 and Plate 2).

The lowest d-values of the model simulation are found in high latitudes. Although condensation is an equilibrium process, the isotopic composition of precipitation is not situated on the MWL over the whole temperature range. Low d-values in polar regions are completely in agreement with a vapor source near 30° south or north. Studies with simple Rayleigh type models [*Petit et al.*, 1991; *Johnsen et al.*, 1989; *Ciais et al.*, 1995] have shown that the deuterium excess of subtropical vapor change from 10–12‰ at the origin to 5–8‰ at high latitudes. This is mainly due to the changes of the equilibrium fractionation factors slightly deviating with lower temperatures from a constant relationship. Very low excess values have been measured, for example, at the Antarctic station Argentine Island (d=1‰). However, a low excess possibly might also indicate the admixture of vapor evaporated under quite cold conditions (south of 60°S). Under such circumstances the evaporation is a slow process allowing almost perfect isotopic equilibration and therefore lower d values in the corresponding precipitation. In this study we can not distinguish between the two possible reasons for low d-values in high latitudes, i.e., the condensation process over a wide temperature range or the admixture of vapor from a cold vapor source nearby.

For Antarctica the kinetic fractionation during formation of ice crystals is important. In Figure 7 we plot the deuterium excess for all model grid points over Antarctica versus the corresponding δD-values which correspond in this region to a temperature scale. Although the model seems to be noisier than the observations, there is a good agreement with the existing measurements on snow. Coastal or near coastal data (-150 to -300‰ δD) show quite low d-values of 2–5‰(simulated -2 to +1‰) while the d-values on the East Antarctic ice sheet increase up to a maximum of +18‰ (15‰ in the model).

Besides the global offset of about 2–4‰, the simulated pattern of the deuterium excess is close to the observations, with low d-values in polar regions, an in-

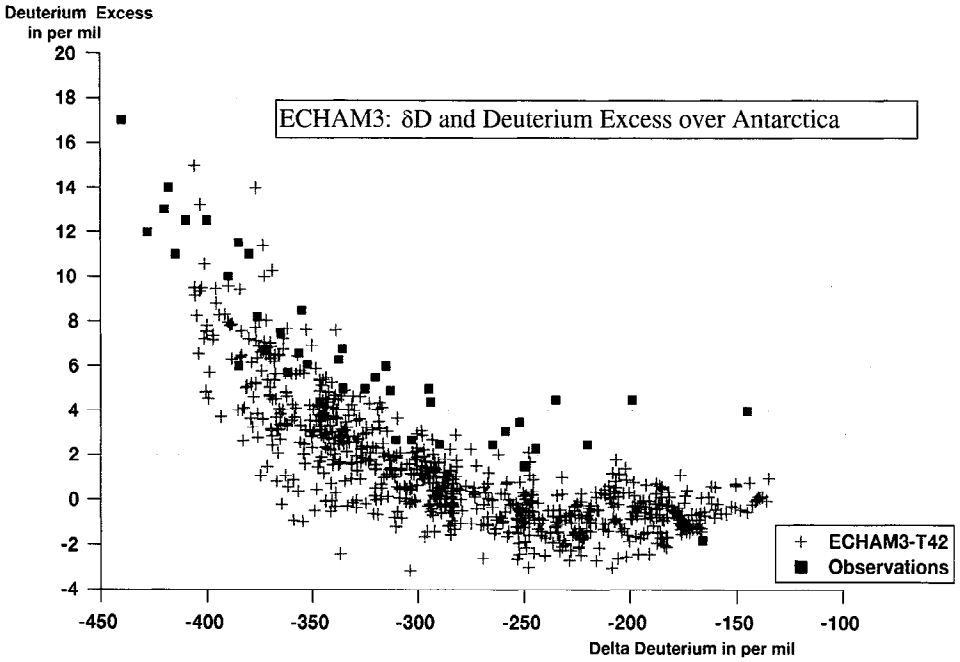

Figure 7. Deuterium excess d in precipitation over Antarctica versus the corresponding δD values simulated by the ECHAM3 T42-control run over 5 years (the pluses represent all grid point results over Antarctica). The observations (squares) are adapted from *Petit et al.* [1991].

crease over the top of the ice sheets, and quite high values over Asia. The second local kinetic effect built into the model, the reevaporation of raindrops below the cloud base, does not considerably influence the simulated deuterium excess. Less than 1% of global precipitation undergoes such an evaporation in the model. Because of the existing deficits of the model simulating even the first-order quantity $\delta^{18}O$ in arid zones, the low modeled excess value in the Sahara cannot clearly be traced back to the nonequilibrium process taking place during reevaporation (see Figure 1). Rather dry conditions prevailing in the Sahara can, in fact, be responsible for the low excess of down to 1‰ simulated there.

3.5. Regional Studies

Recently, a discussion came up on the validity and on the calibration of the δ-paleothermometer in Greenland [*Cuffey et al.*, 1995; *Johnsen et al.*, 1995]. Under different climate conditions such as the last glacial maximum, many local and nonlocal effects might affect the temperature–isotope relation (for a full discussion see *Jouzel et al.* [1997]). AGCMs were already used to estimate the influence of a glacial climate on the water isotopes [*Jouzel et al.*, 1994; *Charles et al.*, 1994; *Joussaume and Jouzel*, 1993; *Hoffmann and Heimann*, 1997]. Therefore they should fulfill a series of criteria in order to gain confidence in AGCM's responses on boundary conditions different from the present ones. Such criteria are a reasonable simulation of the regional climate and a spatial and seasonal temperature–isotope relation in accordance with today's observations. However, even then, it does not indicate that the model simulates the right pathways and source regions of vapor for present-day conditions. Local forcing factors, such as the temperature effect, are too strong to investigate remaining problems of the modeled vapor transport. Furthermore, there exist many possibilities of two or more model deficits canceling each other. Therefore we investigate here the deuterium excess and its seasonal phase relation to the $\delta^{18}O$ signal as a further test for the modeled vapor source regions. We compare the model results for two regions, western Europe and central Greenland, with observations and with the modeled isotope signal in the subtropical North Atlantic, which presumably is the most important vapor source for both regions.

In the literature the observed annual mean of the deuterium excess and the phase relation between the seasonal cycle of $\delta^{18}O$ and d were used to estimate possible source regions of vapor and their seasonally varying contribution to the precipitation [*Johnsen et al.*, 1989; *Ciais et al.*, 1995]. Unfortunately, the observations of the seasonality of the deuterium excess d are not unambiguous or easy to interpret. A large part of the IAEA stations (about 50%) do not show any seasonality of the excess, while some stations such as the North Atlantic stations Reykjavik (Iceland) and Isfjord (Spitsbergen) show a clear antiphasing between $\delta^{18}O$ and d as was already pointed out by *Johnsen et al.* [1989]. However, there are also many stations with a phase lag of approximately 3 months between $\delta^{18}O$ and d, for example at Argentine Island (Antarctic coast) or Vienna. There exist even stations with a clear in-phase relationship between $\delta^{18}O$ and d like the east Asian stations Pohang (Korea), Guilin, and Guiyang (China).

In Figure 8, we show a zoom of the ECHAM results (annual mean accumulation and annual average $\delta^{18}O$) in both model resolutions (T21,T42) over Greenland. The observations are taken from the IAEA stations located along the coast around Greenland and from measurements on firn cores (Greenland ice sheet project 2 (GISP2) ice core [*Stuiver et al.*, 1995], the Expédition Glaciologique Internationale au Groenland (EGIG) traverse [*Fischer et al.*, 1995], the IAEA network [*IAEA*, 1992], and *Anklin and Stauffer* [1994], *Friedmann and Moore* [1995], and *Ohmura and Reeh* [1991]). Obviously, the low-resolution version of the model fails to predict the pronounced low-precipitation area over the northern part of the ice sheet (less than 15 cm/yr observed, as compared to 50 cm/yr simulated in the T21-control over central Greenland). Furthermore, the simulated temperatures are approximately 15°C higher than the observed temperatures. Both deficiencies can at least partly be attributed to the poor resolution of the ice sheet topography which is underestimated by more than 1000 m in the T21 resolution. Nevertheless, the isotopes almost show the observed structure with the most depleted snow only 8‰ larger than observed. Again the T42 version yields a much more satisfying result with a low-accumulation area situated on the top of the ice-sheet (≈10 cm/yr) which is in excellent agreement with published accumulation maps [*Ohmura and Reeh*, 1991]. Near Summit the simulated isotope values are only 2‰ higher than the observed ones (-34‰simulated), while the predicted temperatures are 1°C–3°C lower compared to the observations. Also, the so-called Lee effect of the water isotopes, which is responsible for the asymmetric spatial gradient of the isotopes over Greenland, is reproduced by the ECHAM. As documented by the measurements of the EGIG traverse, the spatial slope of the δ-values from the western coast to the center of Greenland is smoother than at the eastern coast where the already strongly depleted vapor advected from the West over the top of the ice sheet causes lower $\delta^{18}O$-values at corresponding heights [*Fischer et al.*, 1995; *Johnsen et al.*, 1989]. Consequently, the calculated spatial gradient $\delta^{18}O$-T for Greenland is in excellent agreement with the observations ($0.69\frac{‰}{°C}$ with r=0.92 compared with $0.69\frac{‰}{°C}$ [*Johnsen et al.*, 1989]).

Although these results look satisfying, we like to point out that the simulation of the regional spatial slopes does not necessarily indicate that the vapor source regions are correctly determined by the model. Figure 9 shows the modeled annual cycle of $\delta^{18}O$ and of the deuterium excess over central Greenland. The $\delta^{18}O$-

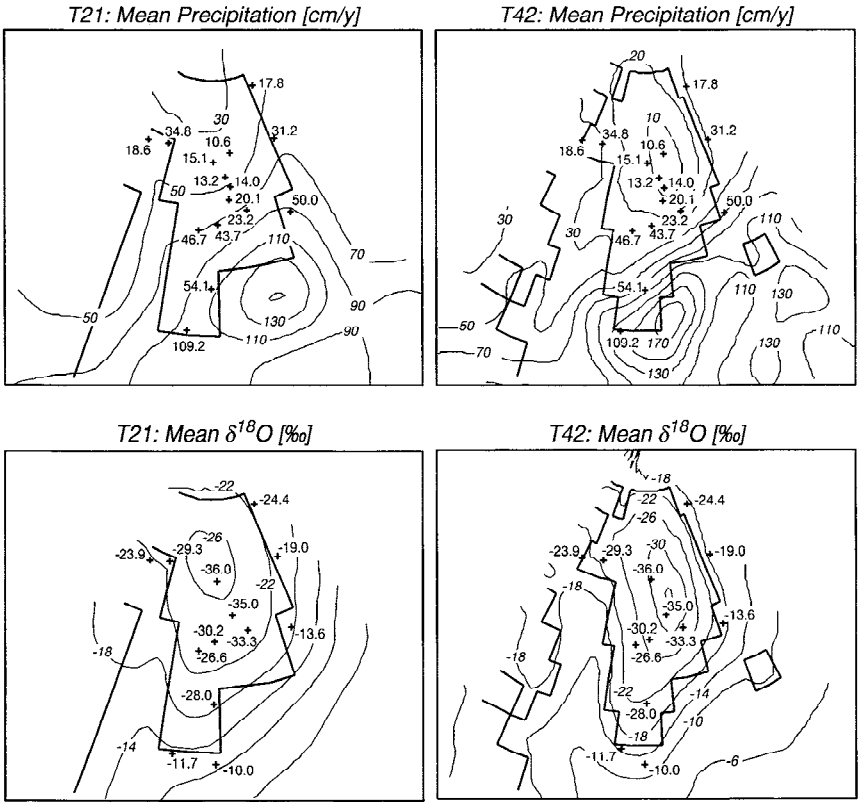

Figure 8. Simulated precipitation, observed accumulation rates, and corresponding $\delta\,^{18}O$ values over Greenland for T42-control and T21-control. The observations are given as numbers at the sample sites (pluses).

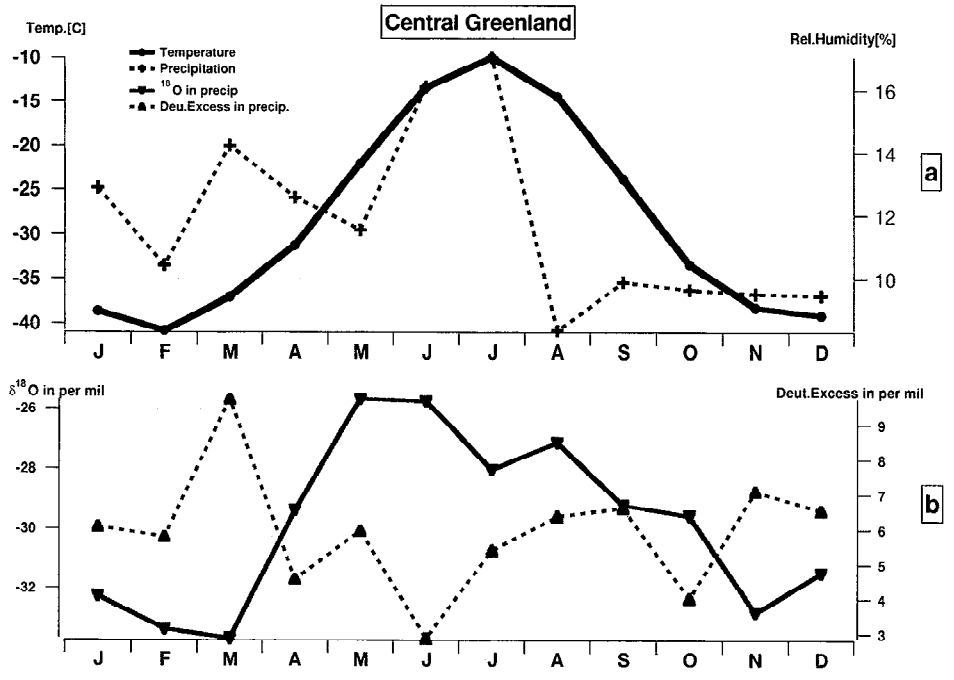

Figure 9. T42-control run over 5 years: annual cycle of precipitation, surface air temperature (a), ^{18}O and deuterium excess of precipitation (b) over central Greenland (45°– 30°W ; 80 °– 70°N). The amplitude of the ^{18}O cycle is about 9‰ with a maximum already reached in June. There is no clear cycle of the deuterium excess over Greenland.

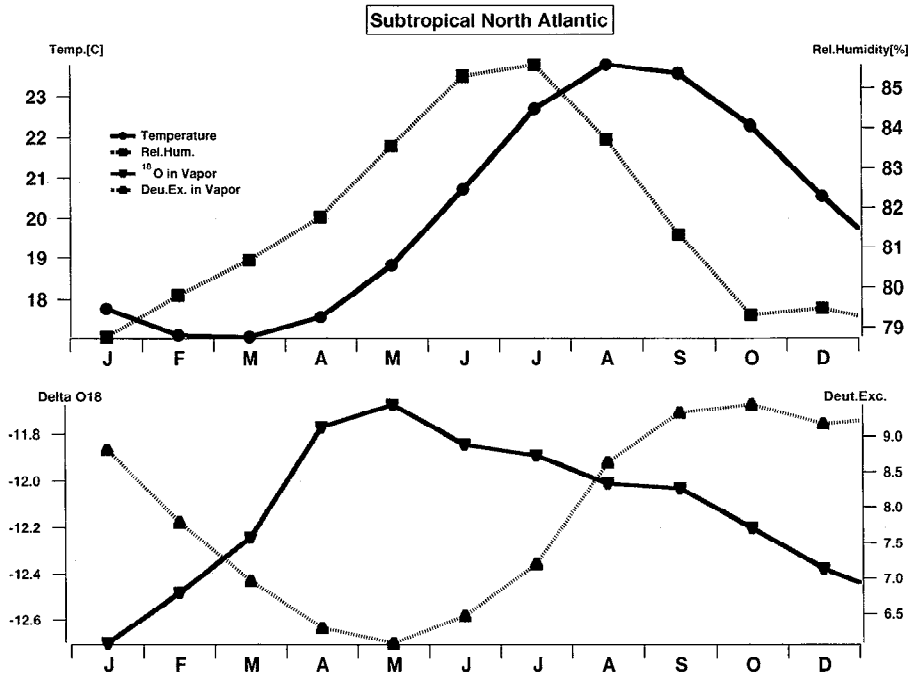

Figure 10. T42-control run over 5 years: Annual cycle of surface air temperature, relative humidity (a), ^{18}O, and deuterium excess of vapor in the lowest model layer (b) over the subtropical North Atlantic (70°W– 10°E; 45–20°N). The deuterium excess lags the ^{18}O signal by about 4 months. Its dependence on the relative humidity and on temperature at the evaporative site is not unique.

value reaches its minimum quite late in March and increases rapidly to the maximal summer value in May. The amplitude of the seasonal cycle amounts to about 8‰ which seems to fit the observations of the central Greenland ice cores (for the Greenland ice core project (GRIP) core see *Hoffmann et al.* [1998]). However, the amplitudes measured in the ice underestimate most probably the original signal in the snow due to the strong diffusion of the isotope signal in the firn during the first years after deposition. Measurements on these uppermost meters of snow gave a peak-to-peak amplitude (highest summer value minus lowest winter value) of 18–20‰ [*Shuman et al.*, 1995], indicating that the simulated amplitude might be considerably too small. Furthermore, the model simulates anomalous low δ-values in midsummer (monthly $\delta^{18}O$ of July is about 2‰ more negative than the June value, although July is the warmest month), systematically appearing in each of the five simulated years although the corresponding temperature and precipitation do not show any such behavior (Figure 9). The model obviously produces such low summer values by advecting isotopically strongly depleted vapor to the top of the ice sheet. This result is in clear contradiction to measurements on firn cores showing a rather regular seasonal cycle of $\delta^{18}O$ without any secondary minima in summer. Also, the observed seasonality of the deuterium excess [*Johnsen et al.*, 1989] with a phase shift of approximately 3 months compared to the $\delta^{18}O$; that is, a maximum of d in early autumn and a minimum in spring is not predicted by the model (Figure 9).

It is important to note that the missing seasonal cycle of d over Greenland is not a general feature of the ECHAM simulation. Figure 10 shows the seasonal cycle of $\delta^{18}O$ and the d-value of the vapor, temperature, and relative humidity on the lowest model level averaged over the subtropical North Atlantic (20°–45°N, 70°W–10°E). This region is usually assumed to be the most important vapor source for the precipitation over Greenland and over western Europe. Unfortunately, there are not many measurements of the isotopic composition of marine vapor [*Craig and Gordon*, 1965]. The simulated values between -12.7‰ and -11.7‰ are well situated in the range spanned by the observations (-10.5‰to -14‰ between 5°N and 35°N in the Pacific). The modeled seasonal cycle of $\delta^{18}O$ in vapor is quite small ($\approx$1.3‰) and is shifted by about 3 months relative to the temperature. Such a shift of the isotopic composition relative to the air temperature (the difference of the maximum in May to the August value amounts only to 0.3‰) could be due either to the relative humidity influencing the δ value of the evaporative flux (see equation 2) or to the dynamics of the regional moisture transport. In particular, the strength of mixing of high-altitude vapor being already quite depleted in the heavier isotopes with vapor of the planetary boundary layer is important. This process controls the extent to which the isotopic composition of vapor above the ocean

surface deviates from the evaporative flux. Therefore a $\delta^{18}O$ signal deviating in its seasonality from the temperature signal is certainly possible. However, there are no measurements available to confirm the predicted shift.

The deuterium excess shows a clear seasonality with a maximum in fall (September–December) and a minimum during spring (April–June). Two quantities primarily affect the kinetic fractionation during evaporation: temperature and humidity (Figure 10). In general, low temperatures at the evaporation site cause slow evaporation in near-isotopic equilibrium, while a low relative humidity causes fast evaporation with a strong kinetic fractionation (and vice versa). Therefore the two seasonal cycles of temperature and relative humidity shown in Figure 10 have opposite effects on the deuterium excess in vapor.

The isotopic composition of precipitation over western Europe is, in fact, strongly affected by the subtropical Atlantic Ocean. Thus the seasonal signal of the deuterium excess follows the signal imposed by the vapor in the source region. Figure 11 shows the simulated seasonal cycle of temperature, precipitation, $\delta^{18}O$, and d (of precipitation) over Europe (all land points from 15°W to 25°E and 60°to 45°N) and the corresponding observations (mean over 28 IAEA stations). The most important climate parameters controlling the isotopic composition at the condensation site, i.e., temperature and precipitation, show roughly the same seasonality and nearly the same mean value (temperature and precipitation of the IAEA stations do not represent a pure regional mean; for our purpose it is only important to know to what extent the simulated and the observed local climate quantities influencing the isotopes agree with each other). Generally, the simulated $\delta^{18}O$ cycle fits the observations although the summer maximum seems to be somewhat too broad. The deuterium excess shows the same seasonality as the excess of the vapor in the source region with a maximum in autumn and a minimum in late spring. This holds although the simulated monthly variability of the deuterium excess is nearly twice as large as the observed variability (about 7‰ are observed). In spite of the high variability the phasing of the deuterium excess cycle in precipitation for many regions is quite a robust result of the model. If there is a seasonal cycle in the model, the simulated d-values lag the first-order quantity $\delta^{18}O$ by 2-3 months.

3.6. Interannual Variations

Interannual variations of the isotopic composition of precipitation, as they are recorded during the last 30 years by the IAEA network, are quite small. They amount approximately 1–3‰ $\delta^{18}O$ in high latitudes and something less in the tropics and subtropics (0.5–1.5‰ $\delta^{18}O$). *Rozanski et al.* [1993] already investigated how these small variations are related to corre-

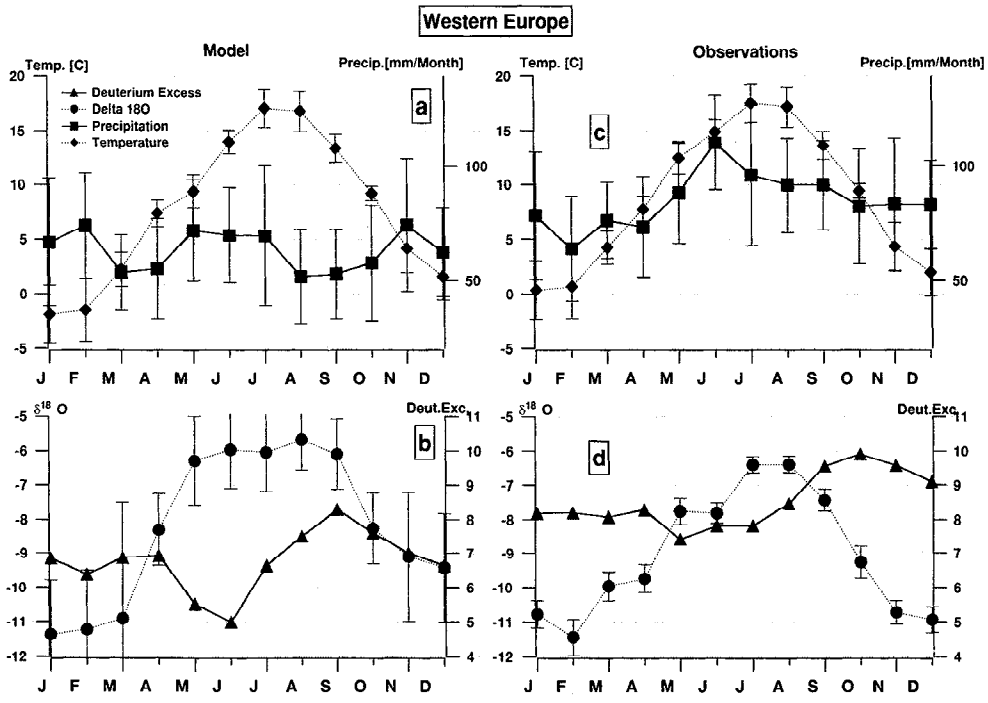

Figure 11. T42-control and IAEA Observations (28 stations): Annual cycle of precipitation (a,c), temperature (a,c), ^{18}O (b,d) and deuterium excess of precipitation (b,d) over western Europe (15°W– 20°E; 60–45°N). The seasonal amplitude of ^{18}O amounts to about 6‰. In correspondence to the observations the model simulates a phase shift of 2–3 months of the seasonal cycle of the deuterium excess compared to ^{18}O.

sponding variations of temperature and precipitation and generally found rather weak correlations. Overall, the highest correlation is found in western Europe. One of the oldest IAEA stations, Vienna, shows an interannual correlation of r=0.6 with a gradient of $\Delta_{\mathrm{IntAnn}}\delta^{18}O/\Delta_{\mathrm{IntAnn}}T$=0.65‰/°C. There are also isotope studies on interannual variations like ENSO (El Niño Southern Oscillation) [*Thompson*, 1993] and the North Atlantic Oscillation [*Barlow et al.*, 1993] in high-resolution ice core records covering several hundred years.

To investigate the interannual variability of the modeled isotope signal, we integrated the coarse resolution version of the ECHAM model forced by observed SSTs (T21-AMIP) over the period 1979–1988. The use of varying sea surface temperatures as lower boundary conditions generally enhances the variability of the model. In particular, over the oceans the atmospheric modeling intercomparison project (AMIP) simulation includes phenomena such as El Niño type variations which are otherwise absent in the averaged climatological SSTs of the control run. We analyzed the results of the 10 year simulation by calculating the monthly anomalies of δ^{18}O, precipitation, and temperature (i.e., a time series of 120 anomalies). In Plates 4 and 5 we show the resulting correlations between the isotope anomalies and the corresponding temperature and precipitation anomalies, respectively. No correlations are plotted in regions where it is not possible to define a full seasonal cycle. This criterion generates missing values in some arid areas like North Africa and Australia. Again, we added the observations of the IAEA to the plot by calculating the correlations for all stations with at least 3 years of measurements. It must be realized, though, that this procedure yields a qualitatively very heterogeneous data set by merging time series from stations with continuous measurements over more than 20 years with short time series.

Generally, the correlation between the δ^{18}O values and the climate parameters temperature T and precipitation P is quite weak (most r values are between +0.4 and -0.4 for the model and for the observations). The correlation might improve slightly if the investigation is restricted to certain seasons in which the ability of the water isotopes to record interannual variability of the local climate parameters T and P increases [*Lawrence and White*, 1991]. The correlation of the isotopes with the temperature r_T is mostly positive, and r_P, the correlation with the precipitation, is negative. This modeled response on interannual climate variations is in agreement with the temperature and the amount effect. The model simulates the highest r_T values (see Plate 4) in the interior of the northern hemisphere continents and over Antarctica where also the seasonal cycle has the largest amplitudes. The observations show a similar behavior with the best correlations between 0.3 and 0.5 over Russia and North America.

In the tropics, there is a clear simulated signal originating from El Niño such as variations in the sea surface temperatures. El Niño is the strongest natural climate variation on the timescale of a few years and shows quasi-periodic behavior with an approximate period of 2-4 years. It is mainly characterized by warm temperature anomalies in the equatorial Pacific around the equator and is accompanied by strong changes in the hydrological cycle over the tropics and subtropics. During an El Niño event the rising branch of the Walker circulation moves with the temperature anomalies from the region of the western Pacific warm pool eastward. This causes heavy anomalous droughts over Indonesia and eastern Australia and produces quite strong convective activity over the equatorial Pacific around the dateline and also over the Indian Ocean [*Ropelewski and Halpert*, 1989]. During an El Niño event the anomalous strong precipitation over the oceans induces anomalous low δ values due to the amount effect. This leads to a negative correlation of the water isotopes with the temperature (see Plate 4) in the affected regions and, consequently, to a quite strong negative correlation with the amount of precipitation (r_P reaches a global minimum of -0.85 near the dateline, see Plate 5). We note that the entire process of shifts of the Walker cell caused by El Niño type tropical SST anomalies and of the accompanying isotope signal is well known [*Cole et al.*, 1993]. It is the basis of using isotope records of tropical corals as an ENSO proxy [*Cole and Fairbanks*, 1990; *Fairbanks and Dodge*, 1979].

Toward higher latitudes the correlation r_P is slowly decreasing, which is roughly in agreement with the observations. Interestingly, there are two regions where we find positive correlations: polar latitudes (i.e., mainly Antarctica and a smaller region near Greenland) and the regions of the subtropical highs offshore of Africa and of North and South America. In polar latitudes, temperature anomalies covary with precipitation anomalies just for thermodynamic reasons. In a region where the temperature effect dominates the isotopic composition of precipitation, positive temperature anomalies thus produce both positive precipitation anomalies and positive isotope anomalies. The signal in the subtropics can be explained regarding the strength of mixing of already depleted air from upper layers with air of the planetary boundary layer. The sinking zones of the subtropical highs are arid regions (see Figure 2b). Here the air typically descending from high altitudes is isotopically more depleted than air on the same height and latitude. In our simulations, this was a clear pattern of the isotopic composition of water vapor (not shown here). Even weak convective activity slows down the sinking movement of depleted air and allows comparable heavy moisture from the ocean surface to accumulate in the lower atmospheric layers. This process might be responsible of covarying precipitation produced in those convective events and positive δ anomalies on latitudes

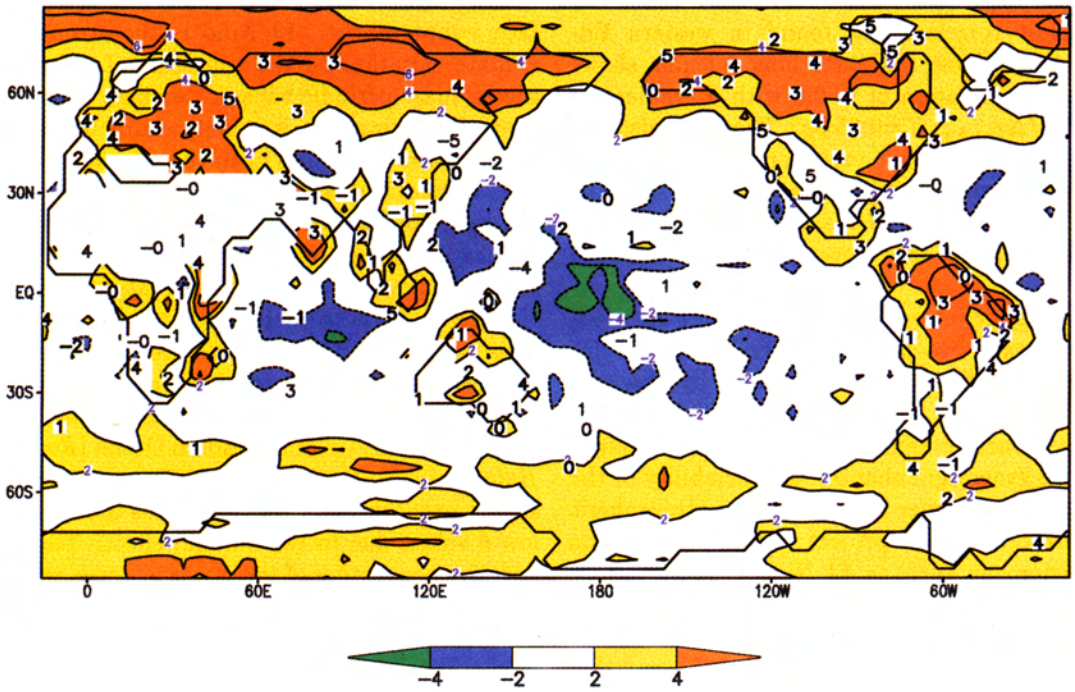

Plate 4. T21-AMIP run over 10 years and IAEA observations: correlation of monthly anomalies of $\delta^{18}O$ and temperature multiplied by 10. The bold numbers denote the calculated correlations for all IAEA stations with at least three seasonal cycles.

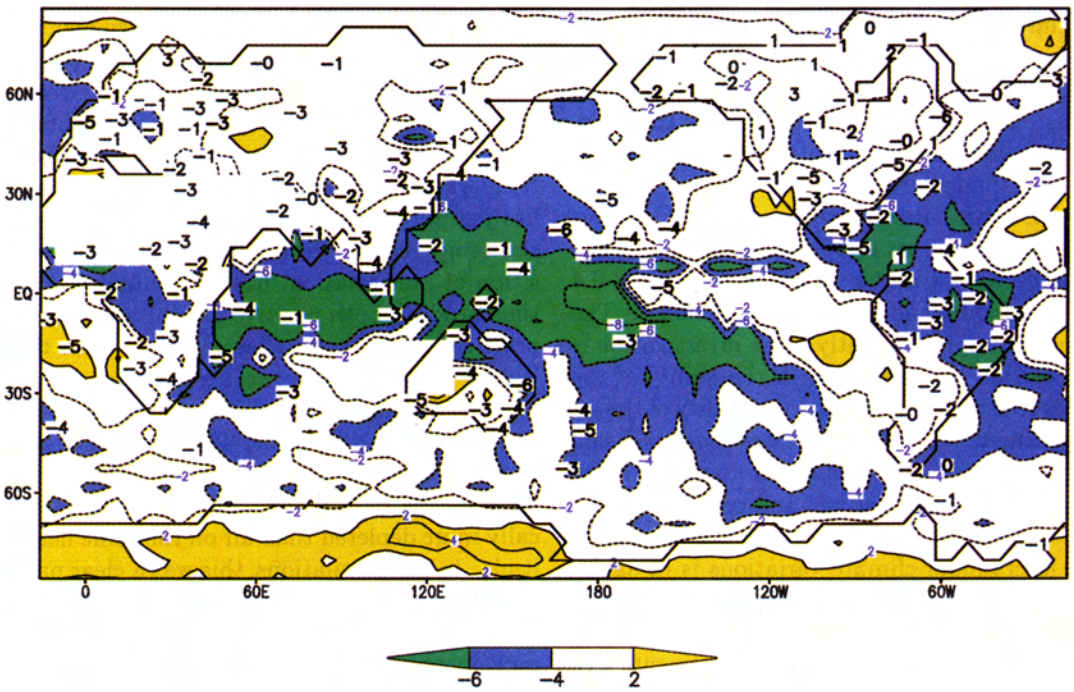

Plate 5. T21-AMIP run over 10 years and IAEA observations: correlation of monthly anomalies of $\delta^{18}O$ and precipitation multiplied by 10. The bold numbers denote the calculated correlations for all IAEA stations with at least three seasonal cycles.

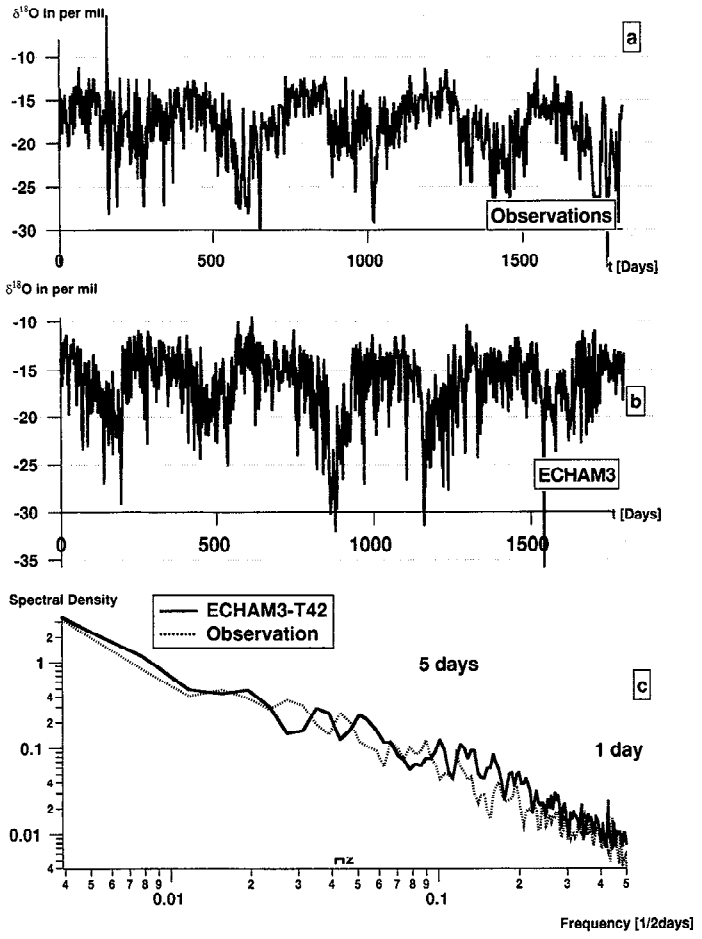

Figure 12. T42-control run over 5 years (a) and observations at Heidelberg, Germany (b) [*Jacob and Sonntag*, 1991]: daily $\delta^{18}O$ of vapor near the ground for 5 years and corresponding power spectra (c). The mean of the observations over the selected 5 years amounts to -17.9 ‰ and the mean of the model results -16.5‰.

where actually the amount effect dominates the isotopic composition of rain (see our discussion above). Nevertheless, the sparse or nonexisting data in these regions cannot confirm the positive correlation r_P neither in Antarctica nor in the subtropical highs.

3.7. Short-Term Variations

Many investigations [*Lawrence et al.*, 1982; *Gedzelman and Lawrence*, 1982; *Jacob and Sonntag*, 1991; *Taylor*, 1972; *Sonntag et al.*, 1983] document the tremendous variability of the isotopic composition of precipitation and of the corresponding vapor on short timescales. In western Europe, for instance, the $\delta^{18}O$ value of vapor can vary within a few days by more than 12‰ which is in fact much more than the seasonal amplitude of approximately 7‰ (see Figure 12 for the observations from Heidelberg, Germany). *Sonntag et al.* [1983] identified changes of the wind direction turning from the West (this means, not so depleted water vapor of marine origin) to the Northeast (continental and very depleted water vapor) to cause at least the largest of the measured variations in water isotopes. There are three processes affecting the isotopic composition of vapor on short timescales. Firstly, the strength of evapotranspiration which establishes a strong vertical gradient of the isotopes in the planetary boundary layer (PBL) within some hours after a rainfall. Secondly, frequency and typical tracks of synoptical weather systems transporting the vapor from its marine origin and control the rainout of air masses, and thirdly, the strength of mixing of air from the PBL with upper layers. In order to get a first, qualitative impression of the short-term variability we compare the daily observations of the isotopic composition of vapor recorded in Heidelberg over more than 10 years [*Jacob and Sonntag*, 1991; *Sonntag et al.*, 1983] with the corresponding model results. The annual mean value (observed mean δ_{Vap}=-17‰ and simulated mean =-16‰) and the seasonal cycle (defined as the difference between July and January: observed and simulated ≈=6‰) are in good agreement. Nevertheless, the simulated variability of the ECHAM on the synoptic timescale (i.e. 1-14 days) clearly exceeds the observed 1 (note the logarithmic scale in Figure 12). It is quite clear from the spectral analysis that the processes controlling the isotopes on timescales of one

month and longer differ from the processes important on the short timescale. Obviously the model simulates the observed variability on longer scales but fails on shorter ones. So far, it is not yet clear which of the three processes mentioned above is responsible for the high variability, but simulation studies with atmospheric tracers in the ECHAM have shown that the model over land simulates a too strong contrast between a rather stratified and stable lower atmosphere and an unstable PBL which allows mixing with upper air (J. Feichter, personnal communication, 1996). In the model, abrupt and frequent changes from stable to unstable situations might produce the overestimated variability on short timescales.

4. Discussion and Outlook

We have shown that the stable water isotopes are well represented in the ECHAM model under today's climate conditions. This itself is an important conclusion with respect to the analysis of runs under different climate conditions such as the last glacial maximum. Furthermore, the analysis of the water isotopes provides a detailed insight in the hydrological cycle as simulated by AGCMs. The recycling of water vapor over Europe as calculated by the model, for instance, was roughly confirmed by our analysis of the seasonally varying continental gradient of the stable water isotopes. However, it is still unclear if the water isotopes can be used for a more precise tuning of the water cycle or not. The overestimated seasonal amplitude of the isotopes over tropical continents (South America, tropical Africa in Plate 1) gives a good example how such a tuning of the water cycle might work. The large amplitude there is due to an overestimation of the amount effect. This contrasts to the tropical oceans where the simulated slope between the precipitation and the δ-value was found to be too flat (in the T42 resolution, see Figure 4). The ECHAM model uses a mass flux scheme in order to describe convective activity which dominates in the tropics [*Tiedtke*, 1989]. The strength of the convection is mainly triggered by the advective flux of vapor at the cloud base. Environmental air is mixed into the rising air of convective towers (entrainment), and vice versa, convectively elevated air, is mixed into the environmental air (detrainment). Certainly, the parameters used to determine the height of convection, the detrainment of rising air, the entrainment of environmental air or the conversion of cloud droplets into precipitation are strongly influencing the vertical gradient of the isotopic composition of vapor and the corresponding precipitation. These parameters are tuned to guarantee a good fit to observations of climate parameters such as precipitation and surface temperatures. They partially differ depending on where the convection takes place (over land or over sea). In the future we will carry through sensitivity studies to test whether the water isotopes can be used to find a best common set of parameters for both the climate parameters and the isotopic composition of precipitation. For such a tuning exercise of AGCM parameters with water isotopes, a situation like over Europe is ideal. Here the density of different types of isotope measurements allow a relatively good control of all components of the hydrological cycle (vapor in different heights, precipitation, river runoff, groundwater).

Obviously, also the parameters inherent to our isotope module have to be tested in additional sensitivity studies. In an extensive study with the GISS model *Jouzel et al.* [1991] show that at least $\delta^{18}O$ and δD of precipitation generally react quite insensitive to changes of the free parameters in the isotope module. This might be different if one compares the simulated results with observations on shorter timescales. Our preliminary look on the simulated variability of the isotopes on the synoptic scale (Figure 12) already suggested that other processes are influencing the day-to-day variations of the water isotopes than those which are important for the monthly means. It remains to be seen if such processes react more sensitive on, for instance, the specified extent to which equilibration between raindrops and vapor within the cloud (chosen 100% in the control simulations) and below the cloud (depending on the type of clouds either 45% or 95% in the control run) occurs.

Furthermore, there exists a dispute as to whether the strong vertical gradient of the isotopic composition of vapor found in the observed few vertical profiles reflects cloud internal processes (equilibration of rain droplets and vapor) or not [*Rozanski and Sonntag*, 1982; *Taylor*, 1984]. In the latter case, the gradient rather reflects the contrasts of air masses above the PBL already been subjected to several condensation processes and vapor within the PBL which is isotopically more homogeneous. In fact, the ECHAM simulated vertical isotopic gradients in rough agreement with the observations (not shown in this paper). We will have to clarify which of the proposed mechanisms are responsible for the steep gradient, and if the simulated gradient is sensitive to the parameters chosen for the isotope module. In all our sensitivity studies done so far, we made the observation that all parameters directly influencing the isotopes are of secondary importance (for example, in one sensitivity study we chose a constant, temperature independent fractionation coefficient α in contrast to the control run). On the contrary, the strength of entrainment and detrainment in convective systems was a first-order process for the simulated vertical gradient in the model.

The three isotope modules in AGCMs existing until now are differing in many aspects. It is beyond the scope of this paper to compare the three models in detail. However, we would like to point out some prominent features differing in the models. The GISS and the LMD model transport the water isotopes proportional to the fluxes of atmospheric moisture (the first by means of a so-called " slope scheme " and the second by means

of an " upstream " scheme). On the contrary, the advective transport in the ECHAM model uses a scheme which is working independently for moisture and for the corresponding water isotopes. The transport in these models is calculated relative to the air instead of to the atmospheric moisture. The ECHAM model uses a semi-Lagrangian transport scheme. It was suggested by *Joussaume and Jouzel* [1993] that the problems of the LMD to simulate the extremely low δ-values in precipitation observed over East Antarctica originate from the overestimated diffusity of the upstream scheme (the LMD model simulated a $\delta^{18}O$ of precipitation about 20‰ heavier in the annual mean than observed in this region). Apparently, only the GISS and the ECHAM models are able to build up the extreme gradients in the isotopic composition from the Antarctic coast to the top of the ice sheet. Both the GISS and the LMD model simulated an excessive spatial variability when trying to transport the water isotopes relative to air instead of a transport relative to water vapor. Although some of the isotope quantities discussed in this paper, such as the seasonal amplitude or the deuterium excess (see Plate 2 and Figure 7) are spatially quite noisy, the ECHAM model simulates isotope values still in agreement with the observed spatial variability by a semi-Lagrangian transport relative to air. Furthermore, both the GISS and the ECHAM models are using a mass flux scheme in order to describe convective cloud formation, whereas the LMD uses an advective adjustment scheme which makes it much more difficult to compute condensation temperatures and mass transport essential for the water isotopes in convective systems. As was already mentioned by *Joussaume and Jouzel* [1993], such a scheme produces a strong vertical diffusion of the water isotopes in vapor. This effect might be responsible for the vanishing linear relationship between the temperature and the δ-value already above 0°C, whereas the GISS and the ECHAM (see Figure 3) simulated a linear relation up to about 15°C in better agreement with the observations. A further correspondence of the GISS and the ECHAM models is the spatial distribution of the mean deuterium excess showing in both models a pronounced maximum over central Asia, a decrease of the excess toward higher latitudes with lowest values around the Antarctic coast and a local maximum again over the top of the East Antarctic ice sheet. A detailed intercomparison of the existing isotope models is needed in order to find out how the different model properties (transport scheme, convective cloud scheme) affect the water isotopes.

There were mainly two purposes of our investigation on the interannual timescale. Firstly, an extension of the temporal domain obviously provides more opportunities to test the model simulations against observations. Indeed, the ECHAM was able to reproduce the observed (but weak) relation between the isotopes and precipitation and temperature on the interannual timescale. The strongest pattern was a quite strong reaction of the water isotopes on changes of the hydrological cycle in the tropics during El Niño events. This behavior has also been mentioned in a comparable study performed with the GISS model [*Cole et al.*, 1993]. The second aim was to locate regions which possibly react very sensitively to relatively small temperature or precipitation changes. This question is of a very practical nature: Do there exist regions on the globe that might be particularly suitable to detect predicted climate changes by means of water isotope measurements? At least on the basis of our low-resolution T21-AMIP run it is still impossible to recommend high sensitive areas for possible new IAEA stations. This could change if we run the isotope module in a future study under the boundary conditions of a $2\times CO_2$ climate like it has been investigated by many GCM modeling groups. The enhanced concentration of atmospheric greenhouse gases and the assumed accompanying warming might change characteristically the global cycle of the water isotopes. Therefore it is still open if the water isotopes are an attractive tracer to detect climate change or not.

Finally, a global monitoring program of the isotopic composition of large river systems, possibly set up in the near future by the IAEA, might allow a more complete comparison between the observations and the corresponding part of climate models. Because large river systems integrate the isotopic inputs over a huge catchment area, such measurements might be very well suitable to record also small variations in the distribution of water isotopes on a continental-wide spatial scale.

Appendix: River Runoff Scheme

The river runoff scheme solves a simple two-dimensional transport equation for the water content W (in cubic meter) with the locally calculated AGCM runoff R as sources and the runoff into the Ocean S as sinks. We have

$$\frac{\partial W_{i,j}}{\partial t} = Adv_{i,j} + R_{i,j} - S_{i,j} \qquad (A1)$$

$S_{i,j}$ is $\neq 0$ only at coastal points. The model grid used here is the same as the ECHAM grid; the time step is 4 hours. $Adv_{i,j}$ is the sum of the transport over the four grid sides of a box (i, j). It is calculated by a simple upstream formulation (here for the zonal component):

$$Adv_{i,j} \rightarrow {}_{i+1,j} = \begin{cases} u_{i,j} W_{i,j} & \text{if } u_{i,j} \geq 0 \\ u_{i,j} W_{i+1,j} & \text{if } u_{i,j} < 0 \end{cases} \qquad (A2)$$

where $u_{i,j}$ is the zonal velocity depending on the slope of the orography $h_{i,j}$:

$$u_{i,j} = \frac{c}{\Delta x}\left[\frac{h_{i,j} - h_{i+1,j}}{\Delta x}\right]^{\alpha} \qquad (A3)$$

Δx is the models zonal distance between the grid points. A corresponding formulation holds for $v_{i,j}$. Both c, which is an empirical velocity, and α are tuned in order to yield for some of the largest rivers a good correspon-

dence to the observations. The actual difficulty is to define an orography which describes correctly the catchment areas of the various rivers. Unfortunately, the orography of the ECHAM model is spectrally adapted and cannot be taken for these purposes. For more details, see *Sausen et al.* [1994].

The quantity discussed in the text is the coastal river runoff $S_{i,j}$ for both water isotopes and for "normal" water. The isotopic runoff calculation assumes no evaporative enrichment.

References

Anklin, M. and B. Stauffer, Pattern of annual snow accumulation along a west Greenland flow line: No significant change observed during recent decades, *Tellus Ser. B, 46* 294–303, 1994.

Aristarain, A.J., J. Jouzel, and M. Pourchet, Past Antarctic Peninsula climate (1850–1980) from an ice core isotope record, *Clim. Change, 8*, 69–89, 1986.

Arpe, K., L. Bengtsson, L. Dümenil, and E. Roeckner, The hydrological cycle in the ECHAM3 simulations of the atmospheric circulation, in *Global Precipitations and Climate Change*, edited by M. Desbois and F. Desalmand, volume 26 of *NATO ASI Ser.*, pp. 361–377, Springer-Verlag, New York, 1994.

Bariac, T., J. Gonzalez-Dunia, F. Tardieu, D. Tessier, and A. Mariotti, Variabilité spatiale de la composition isotopique de l'eau (^{18}O,^{2}H) au sein des organes des plantes aeriennes,1, Approche en conditions controlées, *Chem. Geol., 115*, 307–315, 1994a.

Bariac, T., J. Gonzalez-Dunia, F. Tardieu, D. Tessier, and A. Mariotti. Variabilité spatiale de la composition isotopique de l'eau (^{18}O,^{2}H) dans le continuum sol-plante-atmosphére, *Chem. Geol., 115*, 317–333, 1994b,

Barlow, L.K., J.W.C. White, R.G. Barry, and P.M. Grootes, The North Atlantic oscillation signature in deuterium and deuterium excess in the Greenland ice sheet project 2 ice core, 1840–1970, *Geophys. Res. Lett., 20*(24),2901–2904, 1993.

Charles, C.D., D. Rind, J. Jouzel, R.D. Koster, and R.G. Fairbanks, Glacial-Interglacial changes in moisture sources for Greenland: Influence on the ice core record of climate, *Science, 263*, 508–511, 1994.

Ciais, P., J.W.C. White, J. Jouzel, and J.R. Petit, The origin of present day antarctic precipitation from surface snow deuterium excess data, *J. Geophys. Res., 100*, 18,917–19,827, 1995.

Cole, J.E. and R.G. Fairbanks, The southern oscillation recorded on the oxygen isotopes of corals from Taraw atoll. *Paleoceanography*, 5:669–683, 1990.

Cole, J.E., D. D.Rind, and R.G. R.G.Fairbanks, Isotopic responses to interannual variability simulated by an AGCM, *Quat. Sci. Rev., 12*, 387–406, 1993.

Craig, H., Standard for reporting concentrations of deuterium and oxygen-18 in natural water, *Science, 133*, 1833–1834, 1961.

Craig, H. and L.I. Gordon, *Deuterium and oxygen-18 variations in the Ocean and the Marine Atmosphere*, Cons. Naz. delle Ric., Lab. di Geol. Nucl., Triest, Italy, 1965.

Cuffey, K. M., G. D. Clow, R.B. Alley, M. Stuiver, E.D. Washington, and R.W. Saltus, Large Arctic temperature change at the glacial-holocene transition. *Science, 270*, 455–458, 1995.

Dansgaard, W., Stable isotopes in precipitation, *Tellus, 16* 436–468, 1964.

Dümenil, L., K. Isele, H.-J. Liebscher, U. Schröder, M. Schumacher, and K. Wilke, Discharge data from 50 selected rivers for GCM validation, *Tech. Rep. 100*, Max-Planck Inst. für Meteorol., Hamburg, Germany, 1993.

Fairbanks, R.G. and R.E. Dodge, Annual periodicity of the O-18/O-16 and C-13/C-12 ratios in the coral Monastrea annularis, *Geochim. Cosmochim. Acta, 43*, 1009–1020, 1979.

Fischer, H., D. Wagenbach, M. Laternser, and W. Haeberli, Glacio-meteorological and isotopic studies along the EGIG line, central Greenland, *J. Glaciol., 41*(139), 515–527, 1995.

A. Friedmann and J.C. Moore, A 1200-year record of accumulation from northern Greenland, *Ann. Glaciol., 21*, 19–25, 1995.

Fritz, P., Rivers, In *Stable Isotope Hydrology*, vol. 210, pp. 203–219. Int.At.Energ.Agency, Vienna, Austria, 1981.

Gat, J.R., Groundwater, In *Stable Isotope Hydrology*, vol. 210 of *Tech. Rep. Ser.*, pp. 223–240, Int.At.Energ.Agency, Vienna, 1981.

Gat, J.R. and I. Carmi. Evolution of the isotopic composition of atmospheric waters in the Mediterranean Sea area, *J. of Geophys. Res., 75*, 3039, 1970.

Gat, J.R. and E. Matsui, Atmospheric water balance in the Amazon Basin: An isotopic evapotranspiration model, *J. Geophys. Res., 96*, 179–188, 1991.

Gedzelman, S.D. and J.R. Lawrence, The isotopic composition of cyclonic precipitation, *J. Appl. Meteorol., 21*, 1385–1404, 1982.

Grootes, P.M., M. Stuiver, L.G. Thompson, and L.G. Mosley-Thompson, Oxygen isotope changes in tropical ice, Quelcaya, Peru, *J. Geophys. Res., 94*, 1187–1194, 1989.

Hitchon, B. and H.R. Krouse, Hydrogeochemistry of the surface waters of the Mackenzie River drainage basin, Canada, III, Stable isotopes of oxygen, carbon and sulphur, *Geochim. Cosmochim. Acta, 36*, 1337–1357, 1972.

Hoffmann, G. and M. Heimann, Water isotope modeling in the Asian monsoon region, *Quat. Int., 37*, 115–128, 1997.

Hoffmann, G., M. Stievenaard, J. Jouzel, J.W.C. White, and S.J. Johnsen, The deuterium excess record from central Greenland: Modelling and observations, in *International Symposium on Isotope*

Techniques in the Study of Past and Current Environmental Changes in the Hydrosphere and the Atmosphere, Int.At.Energ.Agency,Vienna, Austria, in press. 1998.

Int.At.Energ.Agency, Statistical Treatment of Data on environmental isotopes in precipitation, *Tech. Rep. 331*, Vienna, Austria, 1992, 1994,

Jacob, H. and C. Sonntag, An 8-year record of the seasonal variation of ^2H and ^{18}O in atmospheric water vapour and precipitation at Heidelberg, *Tellus Ser. B, 43*, 291–300, 1991.

Jaeger, L. Monatskarten des Niederschlags für die ganze Erde, *Tech. Rep. 139*, D. Wetterdienst, Offenbach, Germany, 1976.

Johnsen, S. J., D. Dahl-Jensen, W. Dansgaard, and N. Gundestrup, Greenland palaeotemperatures derived from GRIP bore hole temperature and ice core isotope profiles, *Tellus Ser.B, 47*, 624–629, 1995.

Johnsen, S.J., W. Dansgaard, and J.W.C. White. The origin of Arctic precipitation under present and glacial conditions, *Tellus Ser.B, 41*, 452–468, 1989.

Joussaume, J., R. Sadourny, and J. Jouzel, A general circulation model of water isotope cycles in the atmosphere, *Nature, 311*, 24–29, 1984.

Joussaume, S., and J. Jouzel, Paleoclimatic tracers: an investigation using an atmospheric general circulation model under ice age conditions, 2, water isotopes, *J. Geophys. Res., 98*, 2807–2830, 1993.

Jouzel, J. and L. Merlivat, Deuterium and oxygen 18 in precipitation, modelling of the isotopic effects during snow formation, *J. Geophys. Res., 89*, 11,749–11,757, 1984.

Jouzel, J., G.L. Russell, R.J. Suozzo, R.D. Koster, J.W.C. White, and W.S. Broecker, Simulations of the HDO and $H_2^{18}O$ atmospheric cycles using the NASA GISS general circulation model: The seasonal cycle for present-day conditions, *J. Geophys. Res., 92*, 14,739–14,760, 1987.

Jouzel, J., Koster R.D., R.J. Suozzo, G.L. Russsel, J.W.C. White, and W.S. Broecker, Simulations of the HDO and $H_2^{18}O$ atmospheric cycles using the NASA GISS GCM: Sensitivity experiments for present-day conditions, *J. Geophys. Res., 96*, 7495–7507, 1991.

Jouzel, J., Koster R.D., Suozzo R.J., and Russell G.L, Stable water isotope behavior during the last glacial maximum: A general circulation model analysis, *J. Geophys. Res., 99*, 25,791–25,801, 1994.

Jouzel, J., and R. D. Koster. A reconsideration of the initial conditions used for stable water isotope models, *J. Geophys. Res., 101*, 22,933–22,938, 1997.

Jouzel, J., et. al., Validity of the temperature reconstruction from water isotopes in ice cores, *J. Geophys. Res., 102*, 26471–26487, 1997.

Lawrence, J.R., S.D. Gedzelman, J.W.C. White, D. Smiley, and P. Lazarov, Storm trajectories in eastern US. D/H isotopic composition of precipitation, *Nature, 296*, 638–640, 1982.

Lawrence, J.R., and J.W.C. White, The elusive climates signal in the isotopic composition of precipitation, in *Stable Isotope Geochemisrty: A Tribute to Samuel Epstein*, edited by H.P., Taylor, and J.R., ONeil, and I.R., Kaplan, vol. 3, pp. 169–185. The Geochem. Soc., 1991.

Legates, D.R., and C.J. Willmott, Mean seasonal and spatial variability in gauge corrected global precipitation, *J. Climat., 10*, 111–127, 1990.

Majoube, M., Fractionnement en oxygene 18 entre la glace et la vapeur d'eau, *J. Chem. Phys., 68*, 625–636, 1971a.

Majoube., M., Fractionnement en oxygene 18 et en deuterium entre l'eau et sa vapeur, *J. Chem. Phys., 10*, 1423–1436, 1971b.

Merlivat, L. and J. Jouzel, Global climatic interpretation of the deuterium–oxygen 18 relationship for precipitation, *J. of Geophys. Res., 84*, 5029–5033, 1979.

Merlivat, L., Molecular diffusivities of $H_2^{16}O$, $HD^{16}O$, $H_2^{18}O$ in gases, *J. Chem. Phys., 69*, 2864, 1978.

Roeckner,E. et. al., Simulation of the present-day climate with the ECHAM Model: impact of model physics and resolution, *Tech. Rep. 93*, Max-Planck Inst. für Meteorol., 1992.

Modellbetreuungsgruppe, The ECHAM3 atmospheric general circulation model, *Tech. rep. 6*, Max-Planck Inst. für Meteorol., Hamburg, Germany, 1994.

Ohmura, A. and N. Reeh, New precipitation and accumulation maps for Greenland, *J. Glaciol., 37*(125), 140–148, 1991.

Petit, J.R., J.W.C. White, N.W. Young, J. Jouzel, and Y.S. Korotkevitsch, Deuterium excess in recent Antarctic snow, *J. Geophys. Res., 96*, 5113–5122, 1991.

Putnins, P., The climate of Greenland, in , *Climates of the Polar Regions*, edited by Orvig, S., vol. 14, *World Survey of Climatology*, pp. 3–128. Elsevier Science, New York, 1970.

Rasch, P.J. and D.L. Williamson, Computational aspects of moisture transport in global models of the atmosphere, *Q. J. R. Meteorol. Soc.*, 116, 1071–1090, 1990.

Ropelewski, C.F. and M.S. Halpert, Precipitation patterns associated with the high index phase of the southern oscillation, *J. Clim.*, 2, 268–284, 1989.

Rozanski, K. and C. Sonntag, Vertical distribution of deuterium in atmospheric water vapour, *Tellus, 34*, 135–141, 1982.

Rozanski, K., C. Sonntag, and K.O. Münnich, Factors controlling stable isotope composition of European precipitation, *Tellus, 34*, 142–150, 1982.

Rozanski, K., Deuterium and ^{18}O in European groundwater, Links to atmospheric circulation in the past,

Chem. Geol., 52, 349–363, 1985.

Rozanski, K., L. Araguás-Araguás, and R. Gonfiantini, Isotopic patterns in modern global precipitation, in *Climate Change in Continental Isotopic Records*, edited by P.K. Swart, and K.C. Lohmann, and J. MacKenzie, and S. Savin, vol. 78, *Geophys.Monograph Ser.*, pp. 1–37. AGU, Washington, D.C., 1993.

Russell, G.L and J.R. Miller. Global river runoff calculated from a global atmosphere general circulation model, *J. Hydrol., 117*, 241–254, 1990.

Salati, E., A. Dall'Olio, E. Matsui, and J.R. Gat, Recycling of water in the Amazon Basin: An isotopic study, *Water Resour. Res., 15*, 1250–1257, 1979.

Sausen, R., S. Schubert, and L. Dümenil, A model of river runoff for use in coupled atmosphere-ocean models, *J. Hydrol., 115*, 337–352, 1994.

Schulz, J.-P., L. J. Dümenil, J. Polcher, C.A. Schlosser, and Y. Xue. Land surface energy and moisture fluxes: comparing three models, *Tech. Rep. 221*, Max-Planck InstI für Meteorol., Hamburg, Germany, 1997.

Schwerdtfeger, W., The climate of the Antarctic, in *Climates of the Polar Regions*, vol. 14, *World Survey of Climatology*, edited by Orvig, S., pp. 253–355, Elsevier Science, New York, 1970.

Shuman, C.A., R.B. Alley, Anandakrishnan, J.W.C. White, and P.M. Grootes, Temperature and accumulation at the Greenland summit: Comparison of high-resolution isotope profiles and satellite passive microwave brightness temperature trends, *J. Geophys. Res., 100*, 9165–9177, 1995.

Siegenthaler, U. and H. Oeschger, Correlation of $\delta^{18}O$ in precipitation with temperature and altitude, *Nature, 285*, 314–317, 1980.

Sonntag , K., K.O. Münnich, H. Jacob, and K. Rozanski, Variations of deuterium and oxygen-18 in continental precipitation and groundwater, and their causes, in *Variations in the global water budget*, edited by F.A. Street-Perrott, pp. 107–124. D. Reidel, Norwell, Mass., 1983.

Stewart, M.K., Stable isotope fractionation due to evaporation and isotopic exchange of falling waterdrops: Applications to atmospheric processes and evaporation of lakes, *J. Geophys. Res., 80*, 1133–1146, 1975.

Stuiver, M., P. M. Grootes, and T. F. Braziunos, The GISP2 $\delta^{18}O$ climate record of the past 16,500 years and the role of the sun, ocean and volcanoes, *Quat. Res., 44*, 341–354, 1995.

Taylor, C.B., The vertical variations of isotopic concentrations of tropospheric water vapour over continental Europe and their relationship to tropospheric structure, Tech. rep. 504, Instit. of Nucl. Sci., Lower Hutt, New Zealand, 1972.

Taylor, C.B., Verical distribution of deuterium in atmospheric water vapour: problems in application to access atmospheric condensation models, *Tellus Ser. B, 36*, 67–72, 1984.

Thompson, L.G., Reconstructing the Paleo ENSO records from tropical and subtropical ice cores, *Bull.Inst.Fr.Etudes Andines, 22*, 65–83, 1993.

Tiedtke, M., A comprehensive mass flux scheme for cumulus parameterization in large scale models, *Mon. Weather Rev., 117*, 1779–1800, 1989.

Wang, X.F., and D. Yakir, Temporal and spatial vatiations in the oxygen-18 content of leaf water in different plant species, *Plant, Cell Environ., 18*,1377–1385, 1995.

White, J.W.C., in Stable hydrogen isotope retios in plants: A review of current theory and some potential applications, *Stable isotopes in ecological research*, edited by Rundel, P.W. and Ehleringer, J.R. and Nagy, K.A., pp. 142–162, Springer-Verlag, New York, 1989.

White, J.W.C., E.R. Cook, J.R. Lawrence, and W.S. Broecker, The D/H ratios of sap trees: Implications for water sources and tree ring D/H ratios, *Geochim. Cosmochim. Acta, 49*, 237–246, 1985.

Zimmermann, U., D. Ehhalt, and K.O. Münnich, Soil water movement and evapotranspiration change in the isotopic composition of the water, in *Isotopes in Hydrology*, pp. 567–585, Int. At. Energ. Agency, Vienna, Austria, 1967.

G Hoffmann, Laboratoire des Sciences du Climat et de l'Environnement (LSCE), CEA Saclay, BGt. 703 - Orme des Merisiers, F - 91191 Gif-sur-Yvette Cedex,(e-mail:hoffmann@lmce.saclay.saclay.cea.fr)

M.Werner, M.Heimann, Max-Planck Institut für Meteorologie, Bundesstr.55, 20146 Hamburg, Germany.(e-mail:werner@dkrz.de; heimann@dkrz.de)

(Received December 18, 1996; revised January 23, 1998; accepted January 29, 1998.)